Batch Heteroazeotropic Rectification of a Low α Mixture under Continuous Entrainer Feeding

G. Modla, P. Lang, B. Kotai, and K. Molnar
Budapest University of Technology and Economics, Dept. of Chemical and Food Engineering,
H-1521 Budapest, Hungary

The separation of a low-relative-volatility, zeotropic mixture in a batch rectifier with a selective entrainer was studied by feasibility and rigorous simulation calculations. The entrainer is the high boiler in the system and forms a binary heteroazeotrope with the low-boiler component. Beside the traditional batch addition, the continuous feeding of the entrainer was also investigated. The feasibility of the heteroazeotropic distillation in a batch rectifier was assessed by a new method, extending the methods published for the batch homoazeotropic distillation. The method is based on the analysis of the map of the possible overall liquid composition profiles, which also contains the heterogeneous liquid boiling envelope. The results obtained for batch addition and continuous feeding of the entrainer are compared. The influence of the most important operational parameters is also studied. The results are presented for the dichloromethane–acetone mixture by using water as a heterogeneous entrainer.

Introduction

For the separation of such mixtures where the two components (***A*** and ***B***) form an azeotrope or the relative volatility ($\alpha_{A,B}$) is near to the unity, a special distillation method must be applied such as the extractive/homoazeotropic (*ED*) or the heteroazeotropic distillation (*AD*). In both cases a third component (entrainer ***E***) is added to the mixture that makes the separation of ***A*** and ***B*** possible without the formation of new azeotropes (*ED*) or by the formation of at least one heteroazeotrope (*AD*).

Batch distillation has always been an important part of the production of seasonal, uncertain, or low-capacity and high-purity chemicals. It is a very frequent separation process in the pharmaceutical industry and in the wastewater units. A comprehensive review of the computer-aided analysis, optimal design, and control of batch distillation was published by Kim and Diwekar (2001).

The simplest and most frequently used batch-distillation configuration is the rectifier. For the more sophisticated configurations, such as the middle-vessel column, very few experimental results have been published. Although in the last few years several theoretical studies have tackled the feasibility, performance, optimal operation, and control of the batch extractive distillation in conventional (Mujtaba, 1999; Ahon and de Medeiros, 2001) and nonconventional column configurations [such as in middle-vessel column, Safrit and Westerberg (1997), Cheong and Barton (1999a,b,c), Warter and Stichlmair (1999), Phimister and Seider (2000), Low and Sorensen (2002), and in the inverted batch column, Düssel and Warter (2000)], to our knowledge, batch extractive distillation (BED) experimental results have been published so far only for the rectifier [for example, Yatim et al. (1993), Lelkes et al. (1998a), Milani (1999)]. This indicates that before the industrial application of these configurations several practical problems must be still solved. By our former BED experiences with continuous entrainer feeding much better results (Lang et al., 1994; Lang et al., 2000b) can be obtained than by the batch addition of ***E***.

Bernot et al. (1990, 1991) developed a simple method to predict the behavior, the feasibility, and the separation sequence of multicomponent batch distillation. Lelkes et al. (1998b) suggested a method for the assessment of the feasibility of the BED when applying continuous feeding of the homogeneous entrainer for the separation of minimum azeotropes. Lang et al. (2000a) extended this method for the BED separation of maximum azeotropes.

Correspondence concerning this article should be addressed to P. Lang.

The batch heteroazeotropic distillation (BAD) is a classic separation method. The entrainer is added to the charge in the batch before the start of the distillation. On the basis of our former favorable experiences obtained with the continuous entrainer feeding, we also studied its feasibility and characteristics for the batch heteroazeotropic distillation.

Lang et al. (1985) simulated batch heteroazeotropic distillation laboratory experiments in two Raschig-ring packed columns for the recovery of *n*-butanol from a mixture water−*n*-butanol−*n*-butyl acetate. In the calculations based on the theoretical plate model (estimation of the HETP value of the packed column), the column holdup was neglected. The quasi-steady state of the column was modeled by the modified Wang-Henke (Lang, 1991) and Block-Hegner (1976) methods. It was found that the removal of *n*-butyl acetate was efficient only in the case where a large part of the organic phase was also refluxed together with the aqueous phase. During this separation step, the phase profile of the column (the plates where two liquid phases appeared) varied.

The recent literature on batch heteroazeotropic distillation is not too extensive. The works of Stichlmair and Joulia and coworkers are all that can be cited. Köhler et al. (1995) presented experimental results of heterogeneous batch distillation. In the book by Stichlmair and Fair (1998) we find only an interesting azeotropic batch-distillation separation scheme for the mixture ethanol−water by using toluene as the entrainer published earlier by Düssel and Stichlmair (1995). The hybrid process consists of three steps: stripping, decantation, and rectification. Warter et al. (1999) published entrainer selection rules for continuous and batch azeotropic distillation.

Rodriguez-Donis et al. (2001a) addressed the synthesis aspects of the heterogeneous batch distillation in a rectifier under a batch addition of the entrainer. The feasibility of the process for the separation of minimum azeotropes was assessed by simplified modeling and later confirmed by rigorous simulation made by means of a commercial batch-process simulator (ProSimBATCH, Prosim SA). They studied six possible reflux policies and stated that by varying the quantity of one of the liquid phases (namely, that of the entrainer−rich phase) in the decanter during the operation, the still path can be favorably modified (such as the number of separation steps can be reduced by steering the still path toward a pure-component vertex). The simulation results were corroborated by laboratory experiments for the separation of the acetonitrile−water mixture by using acrylonitrile (forming a binary heteroazeotrope with water) as a heterogeneous entrainer. They devoted a separate article to summarizing the rules of selecting a heterogeneous entrainer for the separation of azeotropic and close boiling mixtures (Rodriguez-Donis et al., 2001b). The possibility of the continuous feeding of the entrainer was not taken into consideration by these authors.

The aim of this article is to extend the feasibility method of Lelkes et al. (1998b) for a heterogeneous entrainer and to study the continuous heterogeneous entrainer feeding for the separation of a low-relative-volatility (close boiling) mixture by feasibility and rigorous simulation calculations. The separation of the dichloromethane (DCM,***A***)−acetone (***B***) mixture will be investigated by using water as heterogeneous entrainer (***E***), forming a binary heteroazeotrope with component ***A***. The results obtained by the batch addition (BA) and the continuous feeding (CF) of the entrainer are compared. The influence of the most important operational parameters [reflux ratio (R), molar flow rate (F), and quantity (SF) of the entrainer] is also presented.

Feasibility Studies

First the method applied for the assessment of the feasibility is presented, then the results of the feasibility calculations are shown.

Feasibility method

The feasibility method of Lelkes et al. (1998b) elaborated for the BED separation of minimum azeotropes and applied for maximum azeotropes by Lang et al. (2000a) is extended.

The batch heteroazeotropic distillation is usually performed in a batch rectifier (Figure 1a) consisting of three main parts: the condenser with the decanter (LLE-separator), the rectifying section (all stages of the column), and the still. The whole quantity of entrainer (***E***) is added in batch to the binary charge (***A-B***) before the start of the distillation.

The overhead vapor of composition $\boldsymbol{y}_2$ is totally condensed into two equilibrium liquid phases: an entrainer−lean phase of composition $\boldsymbol{x}'_1$ and an entrainer−rich phase of composition $\boldsymbol{x}''_1$. The molar ratio of the liquid phases in the decanter is given by the lever rule (i is the component index)

$$\phi = \frac{L''_R + D''}{L'_R + D'} = \frac{x'_{1,i} - y_{2,i}}{y_{2,i} - x''_{1,i}} \tag{1}$$

The overall reflux ratio is given by

$$R = \frac{L^0_R}{D^0} = \frac{L'_R + L''_R}{D' + D''} \tag{2}$$

The distillate is usually withdrawn from only one of the two liquid phases. If the distillate consists of pure entrainer−lean phase ($'$), in this case $D'' = 0$ and $\boldsymbol{x}^0_D = \boldsymbol{x}'_D$.

The overall reflux composition becomes fixed if the value of R is specified and $\boldsymbol{x}^0_R$ can be calculated by the lever rule. If a high enough reflux ratio can be ensured by returning all the entrainer−rich phase onto the top tray of the column as reflux, one-phase reflux is applied, that is, $L'_R = 0$, $L^0_R = L''_R$, and $D^0 = D'$. In this case, $R = \phi$ and the composition of the reflux is $\boldsymbol{x}^0_R = \boldsymbol{x}''_1$. If the entrainer−rich phase does not provide a sufficient reflux flow, one part of the entrainer−lean phase is also returned as a reflux, that is, $L'_R > 0$, $L^0_R = L'_R + L''_R$. In this case, $R > \phi$, and the overall reflux composition $\boldsymbol{x}^0_R$ lies between $\boldsymbol{x}''_1$ and $\boldsymbol{y}_2$ on the tie-line.

In the limiting case of $R = \infty$, the reflux composition equals that of the top vapor ($\boldsymbol{x}^0_R = \boldsymbol{y}_2$) and the overall liquid composition ($\boldsymbol{x}^0$) profile of the column follows a residue curve in the case of a packed column, or a distillation line in the case of column containing (theoretical) plates, respectively. For the determination of the residue-curve map of a ternary heterogeneous mixture, the trajectory of the overall composition ($\boldsymbol{x}^0$) of all coexisting liquid phases for the simple distillation still must be calculated (Pham and Doherty, 1990). The

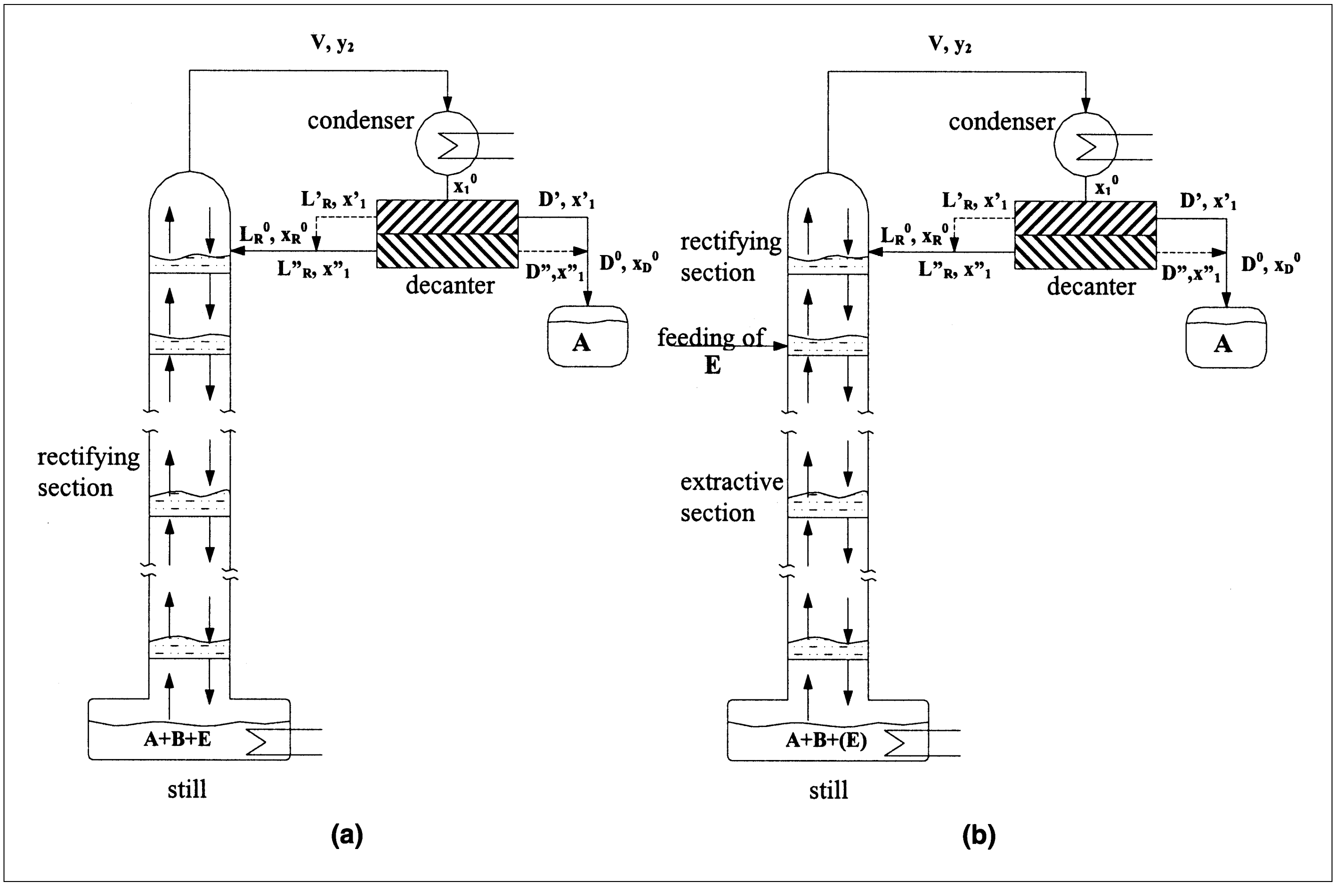

Figure 1. Batch heteroazeotropic distillation column.

(a) Conventional (batch addition of *E*); (b) continuous feeding of *E*. The condensate (x_1^0) can be heterogeneous and it can be separated into an *E*-lean (′) and an *E*-rich (″) liquid phase. In the case of continuous entrainer feeding, the column contains not only a rectifying but also an extractive section.

residue-curve is calculated by

$$\frac{dx^0}{d\xi} = (x^0 - y^*) \tag{3}$$

where ξ denotes dimensionless (warped) time.

If continuous entrainer feeding is applied, the column (Figure 1b) contains two different sections: stages above the feed stage (rectifying section) and stages from the feed plate to the lowest plate of the column labeled extractive section.

The feasibility method is based on the analysis of the still path on the map of possible column-section profiles. The profile map contains the heterogeneous liquid boiling envelope (with the tie lines), as well, since the liquid–liquid phase split must be taken into consideration when assessing feasibility.

The method involves the following basic simplifying assumptions:

- Negligible tray holdup (excluding the decanter and the still);
- Quasi-steady state in the column;
- Constant molar overflow.

For the sake of simplicity in the present work we apply two further assumptions, which could be eliminated easily, but which have no fundamental influence on the feasibility analysis:

- Boiling-point liquid entrainer feeding;
- LLE-separation at the boiling point of the condensate.

The separation is immediately feasible if from the actual liquid in the still (of composition x_S^0 located on the still path) under the given operating conditions (R, F/V) a distillate (of composition $x_{D,\text{spec}}^0$) that can be produced that satisfies the product quality requirements.

The necessary and sufficient condition of the immediate feasibility is to have at least one possible liquid column composition profile connecting the actual still composition (x_S^0):

- With the point $x_{D,\text{spec}}$ if $x_{D,\text{spec}}$ is located in the homogeneous region (excluding the heterogeneous liquid boiling envelope), or
- With the tie-line passing through $x_{D,\text{spec}}^0$ if $x_{D,\text{spec}}^0$ is on the heterogeneous liquid boiling envelope or in the interior of the heterogeneous region.

The feasible column profile may consist of a rectifying or an extractive profile or an extractive and rectifying profile meeting each other.

The longer the immediate feasibility subsists under the given operating conditions, the longer the feasible still path and the larger the quantity of distillate of the prescribed quality.

Variation in the overall still (reboiler) composition ($\boldsymbol{x}_S^0$) with the time can be calculated from the material balances

$$\frac{d\left(U_S^0 \boldsymbol{x}_S^0\right)}{dt} = F \cdot z - D^0 \boldsymbol{x}_D^0 - \frac{d\left(U_1^0 \boldsymbol{x}_1^0\right)}{dt} \tag{4}$$

where U_S^0 and U_1^0 are the overall molar holdups in the still and the decanter, F and D^0 are the molar flow rates of the entrainer feeding and the distillate. The initial condition is defined by

- The charge composition if no entrainer is added in batch, or
- The composition of the mixture obtained from the charge after the batch addition of the entrainer.

If the holdup of each component is constant in the decanter during the period studied (such as in the case of filling up the decanter with heteroazeotropic mixture before the beginning of a distillation, where the top vapor also has the heteroazeotropic composition and the volumes of both phases are kept constant) or there is no decanter, Eq. 4 simplifies to

$$\frac{d\left(U_S^0 \boldsymbol{x}_S^0\right)}{dt} = F \cdot z - D^0 \boldsymbol{x}_D^0 \tag{5}$$

Equation 5 indicates that the moving of $\boldsymbol{x}_S^0$ is due to two simultaneous movements. It leaves the distillate composition $\boldsymbol{x}_D^0$ (point D) and approaches the entrainer feed composition z (vertex E). The path in the still is restricted by a vector cone swept out by two vectors: $(\boldsymbol{x}_S - \boldsymbol{x}_D^0)$ (which points in the direction away from D) and $(z\text{-}\boldsymbol{x}_S)$ (which points in the direction of vertex E). The path in the still follows a straight line whose direction is given by the relative weights of these two vectors until it reaches a boundary or an edge or the vertex of the triangle.

The overall liquid composition profiles of the sections must be calculated in order to assess the feasibility. Taking into consideration the possibility of the presence of two liquid phases when writing the material balances around an inner theoretical stage j of the given section, we get

$$\boldsymbol{x}_{j-1}^0 = V/L^0(\boldsymbol{y}^* - \boldsymbol{y}) + \boldsymbol{x}_j^0 \tag{6}$$

where V is the molar flow rate of vapor; L^0 is the overall liquid flow rate in the given section; $\boldsymbol{y}^*$ is the vapor composition being in equilibrium in the homogeneous region with $\boldsymbol{x}_j^0$ ($\boldsymbol{x}_j^0 = \boldsymbol{x}_j$), and in the heterogeneous region with $\boldsymbol{x}_j'$ and $\boldsymbol{x}_j''$; and $\boldsymbol{y}$ is the vapor composition calculated from the material balance written around the stage j and stage 1 (consisting of the condenser and the decanter).

Van Dongen and Doherty (1985) suggested the application of a differential equation instead of the finite difference material balance equation (Eq. 6) on the basis of which $\boldsymbol{x}_{j-1}^0$ can be calculated from $\boldsymbol{x}_j^0$. Expanding $\boldsymbol{x}_{j-1}^0$ as a Taylor series about $\boldsymbol{x}_j^0$ and disregarding all but first-order derivatives, we have

$$\boldsymbol{x}_{j-1}^0 = \boldsymbol{x}_j^0 + \frac{d\boldsymbol{x}_j^0}{dh}\Big|_{h=j} \Delta h \tag{7}$$

where $\Delta h = (j-1) - j = -1$ and h denotes dimensionless height.

Substituting Eq. 7 into Eq. 6 allows us to write the following simple differential equation for the calculation of the rectifying and extractive profiles

$$\frac{d\boldsymbol{x}^0}{dh} = \frac{V}{L^0}(\boldsymbol{y} - \boldsymbol{y}^*) \tag{8}$$

By this type of model each theoretical tray can be broken into an infinite number of differential plates distributed over the interval from j to $j-1$, with each performing a differential amount of mass transfer. The independent variable h is associated directly with a plate number, but it can also be related to the depth of the packing of a packed column if the HETP is known.

In Eq. 8 the value of the ratio V/L^0 and that of the function $\boldsymbol{y}(\boldsymbol{x}^0)$ can be calculated for the different sections in the following way

- Rectifying section

$$\frac{V}{L^0} = \frac{R+1}{R} \tag{9}$$

and

$$\boldsymbol{y} = \frac{R}{R+1}\boldsymbol{x}^0 + \frac{1}{R+1}\boldsymbol{x}_D^0 \tag{10}$$

- Extractive section

$$\frac{V}{L^0} = \frac{R+1}{R+(R+1)F/V} \tag{11}$$

and

$$\boldsymbol{y} = \left(\frac{R}{R+1} + \frac{F}{V}\right)\boldsymbol{x}^0 + \frac{1}{R+1}\boldsymbol{x}_D^0 - \frac{F}{V}z \tag{12}$$

For each composition $\boldsymbol{x}^0$ it must be decided whether the liquid is homogeneous or heterogeneous (that is, the given point is in a stable or in a meta-stable region of the triangle). For the heterogeneous region instead of a simple VLE calculation, a VLLE calculation must be performed to determine $\boldsymbol{y}^*$, starting from the given overall liquid composition $\boldsymbol{x}^0$. The VLLE calculation involves determining of the boiling point, the composition of the two liquid phases ($\boldsymbol{x}'$, $\boldsymbol{x}''$), and the relative amount of the two liquid phases ($\phi = L''/L'$). The equilibrium calculations (for the UNIQUAC parameters, see Table 1) are performed by the method of Bril et al. (1974) and involve a reliable stability check.

Feasibility calculations

In this subsection we first present the residue curve map of the mixture and the liquid composition profile of the rectifying section of the column at infinite reflux ratio. Then the maps of possible composition profiles of the extractive and rectifying sections are analyzed at finite reflux ratios. This is followed by an investigation of the influence of the opera-

Table 1. Value of the Parameters Used for the Phase Equilibrium Calculations

(*a*) *Antoine parameters**			
Component	*A*	*B*	*C*
DCM (*A*)	7.08030	1,138.910	231.450
Acetone (*B*)	7.117140	1,210.595	229.664
Water (*E*)	8.071310	1,730.630	233.426
(*b*) *UNIQUAC parameters*			
ij	$u_{ij}-u_{jj}$ (cal/mol)	$u_{ji}-u_{ii}$ (cal/mol)	
A B	−38.324	−129.463	
A E	1,026.403	951.710	
B E	601.610	52.302	

*$\log_{10} p^0 = A - B/(t + C)$, where p^0 vapor pressure (mmHg), t temperature (°C).

Table 2. Sequence of the Cuts for the Different Batch Distillation Regions

Batch Dist. Region	No. of Fractions	Sequence	Boiling Points (°C)
I	3	1st cut: ***A-E*** heteroazeotrope	38.3
		2nd cut: ***A***	39.7
		3rd cut: ***B***	56.2
II	3	1st cut: ***A-E*** heteroazeotrope	38.3
		2nd cut: ***B***	56.2
		3rd cut: ***E***	100.0

tional parameters, ends with a comparison of the batch addition and continuous feeding of the entrainer.

The Residue Curve Map and the Rectifying Profiles at Infinite Reflux Ratio. If for the separation of a low-relative-volatility (close boiling) mixture we apply a selective, heavy entrainer (***E***) forming a binary heteroazeotrope with a more volatile component (***A***), the following residue curve map can be obtained (Figure 2) if we also superimpose the heterogeneous liquid boiling envelope (hlbe).

The stable node of the residue curves is vertex *E*. The unstable node is the azeotropic point (*Az*) located on the *A-E* edge within the heterogeneous region. The liquid mixture of composition *Az* splits into two equilibrium liquid phases (*Az*′, *Az*″). There are two saddle points: vertex *A* and vertex *B*.

By the definition of Ewell and Welch (1945) for the batch distillation region, there are two batch distillation regions, separated by the straight line between *Az* and vertex *B*. (This line is not a simple distillation boundary, since it is crossed by the residue curves.) In both regions the first cut is the ***A-E*** heteroazeotrope (Table 2). If the distillation is started from Region I, the problem of the separation of *A*-B arises again after the removal of the whole quantity of ***E*** with the first cut. Therefore, Region II must be reached by the addition of the entrainer to the binary charge, that is, the azeotropic ratio of components ***E*** and ***A*** must be attained or exceeded, that is, the inequality

$$\frac{SF}{U_{ch} x_{ch,A}} \geq \frac{x_{AZ,E}}{x_{AZ,A}} \tag{13}$$

must be satisfied.

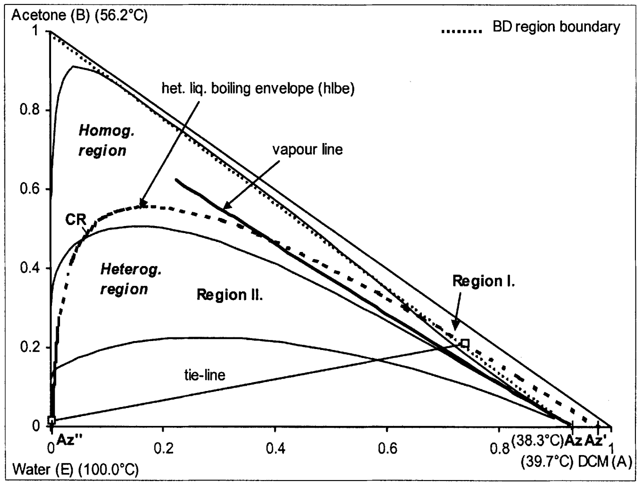

Figure 2. Residue curve-map and heterogeneous liquid boiling envelope for the mixture dichloromethane–acetone + water.

The unstable node of the residue curves is the azeotropic point (*Az*) located on the *AE* edge in the heterogeneous region and which can be reached from anywhere. From the azeotrope by phase splitting an *A*-rich product (*Az*′) can be obtained.

The heterogeneous liquid boiling envelope contains the compositions of the equilibrium liquid phases ($\boldsymbol{x}'$, $\boldsymbol{x}''$) at the boiling point of a heterogeneous mixture of the given overall composition ($\boldsymbol{x}^o$). The points $\boldsymbol{x}^o$, $\boldsymbol{x}'$, and $\boldsymbol{x}''$ are located on a tie line whose endpoints are on the heterogeneous liquid boiling envelope.

In Figure 2 the vapor line and the critical point (*CR*, where the second liquid phase disappears) are also given. The point *Az* is one of the endpoints of the vapor line. The other endpoint of the vapor line is in equilibrium with the point *CR*. For a heterogeneous liquid of composition $\boldsymbol{x}^0$, the equilibrium composition of the vapor phase ($\boldsymbol{y}^*$) is the intersection of the tangent of the residue curve (drawn from $\boldsymbol{x}^0$) with the vapor line. To all points $\boldsymbol{x}^0$ of a tie line, only one equilibrium vapor point ($\boldsymbol{y}^*$) belongs on the vapor line.

If $R = \infty$, the overall composition of the reflux is equal to the top vapor composition ($\boldsymbol{x}_R^0 = \boldsymbol{x}_1^o = \boldsymbol{y}_2$). For the calculation of the rectifying profile from Eq. 8, an equation similar to Eq. 3 can be derived

$$\frac{d\boldsymbol{x}^0}{dh} = (\boldsymbol{x}^0 - \boldsymbol{y}^*) \tag{14}$$

Hence, in the case of $R = \infty$ the rectifying profile follows a simple distillation residue curve and arrives at the vapor line (Figure 3). The residue curves, both starting from the homogeneous point P_a (rc_a) and from the heterogeneous points P_b (rc_b) and P_c (rc_c) approach the vapor line progressively within the heterogeneous region. Each of the rectifying profiles (rp_a, rp_b, and rp_c) calculated from the still compositions just given (P_a, P_b, and P_c) by our method [describing the (continuous) concentration profile of a packed column rather than the discrete profile of a plate column] coincides with the corresponding residue curve. For instance, similar to the residue curve rc_a, the profile rp_a crosses continuously without breaking the heterogeneous liquid boiling envelope.

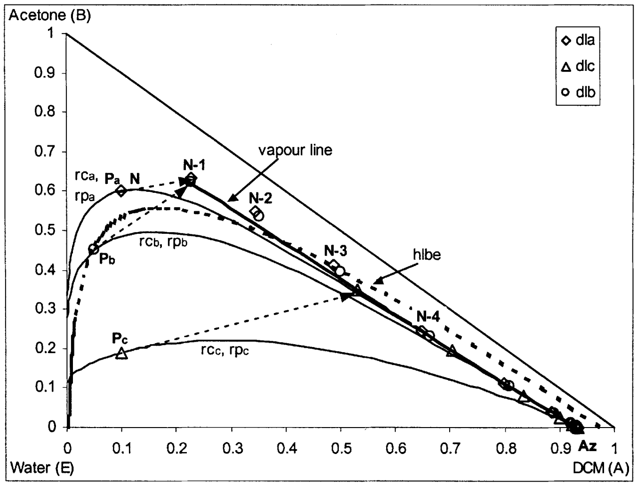

Figure 3. Comparison of the rectifying profiles (*rp*), liquid phase overall plate composition profiles (*dl*) of a heteroazeotropic column with the residue curves (*rc*) at an infinite reflux ratio.

Each rectifying profile coincides with a residue curve in both the homogeneous and heterogeneous region. However, the discrete points of the overall liquid composition profiles, which coincide with the points of the distillation lines, do not remain on the residue curve either in the homogeneous or in the heterogeneous region. From the second successive heterogeneous point the points of the distillation lines are located on the vapor line.

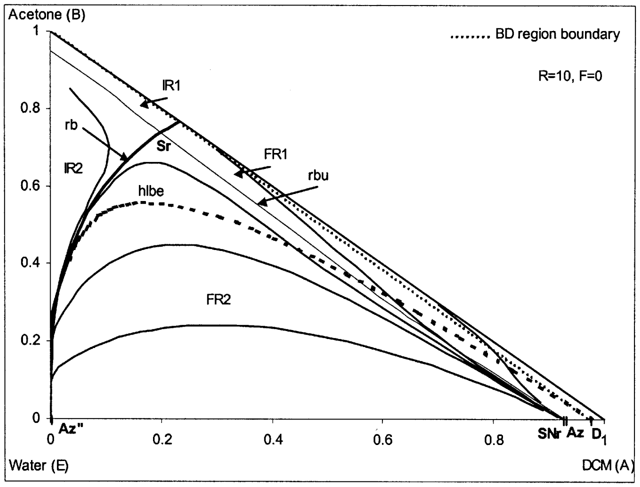

Figure 4. Rectifying profile map at a finite reflux ratio [$R = 10$, $x_D = (0.97, 0.00, 0.03)$].

The stable node of the rectifying profiles (SN_r) is assigned by the overall reflux composition located between *Az* and *Az″* on the *A*-*E* edge. There is a new boundary (*rb*) separating the feasible (FR_1, FR_2) and infeasible regions (IR_1, IR_2). This boundary limits the recovery of component *A*.

If we use the finite difference material balances [as it was done by Rodriguez-Donis et al. (2002)] to calculate the overall composition profile of the rectifying section on the basis of the theoretical plate model, the profile can differ significantly from the residue curve. In this case the profile (consisting of discrete plate compositions x_j^0 ($j = 1 \cdots N$)) follows a distillation line (*dl*).

Two steady-state rigorous calculations were performed under $R = \infty$ for the homogeneous still composition point P_a in order to determine the distillation line. (The method is described later in this article, but here the holdup was neglected.) In the first case (dl_a), we calculated with a high number of stages ($N = 32$) in order to get into the heterogeneous region and to approach the heteroazeotropic point well. Here dl_a did not closely follow rc_a, and already x_{N-1} was located quite far from rc_a on its tangent drawn from point P_a. [The distance from rc_a is significant, since y_N ($= x_{N-1}$) is very different from x_N and rc_a is highly curved.] After crossing the hlbe, the first heterogeneous point (x_{N-4}^0) is not yet located on the vapor line, but the next heterogeneous point (x_{N-5}^0) must already be on it, since $x_{N-5}^0 = y_{N-4}$. After that, dl_a remains on the vapor line and finally approaches well the azeotropic point. In the second case, in order to remain in the homogeneous region, the distillation line was calculated from P_a with a low number of stages ($N = 3$). All three points of the new profile (x_N, x_{N-1}, x_{N-2}) coincided with the corresponding points of dl_a, indicating that the deviation of the distillation lines from the residue curves already exists in the homogeneous region.

Calculations were then carried out for two heterogeneous still compositions (P_b and P_c). When the calculation of dl_b was started from P_b (x_N^0), the composition of the plate just above the still (x_{N-1}^0) was located on the homogeneous part of the vapor line (in the point of intersection of the tangent of rc_b drawn from point P_b and of the vapor line). However, the composition of the next plate (x_{N-2}^0) fell away from the vapor line, since x_{N-1}^0 was not heterogeneous. The composition of the next plate (x_{N-3}^0) was again located in the heterogeneous area, so the composition of the next plate (x_{N-4}^0) was again on the vapor line. The compositions of the plates above plate ($N-4$) remained on the vapor line.

When calculation of *dl* was started from P_c (x_N^0), the composition of the plate adjacent to the still ($x_{\mathrm{N}-1}^0$) was already located on the vapor line (dl_c), since the tangent of rc_c drawn from point P_c cut the vapor line in the heterogeneous area. The compositions of the plates above plate ($N-1$) remained on the vapor line.

The Map of the Possible Concentration Profiles at Finite Reflux Ratios. In the case of a finite reflux ratio, by splitting the heteroazeotrope (*Az*), a distillate (*Az′*) that is richer in *A* than the azeotrope can be withdrawn. In this case the boundary between batch distillation regions I and II is the line between *Az′* and vertex *B* (dotted line in Figure 4) instead of the line $\overline{AzB}$, as it was before. Hence, in this case the following inequality must be satisfied when we choose the amount of the entrainer

$$\frac{SF}{U_{ch}x_{ch,A}} \geq \frac{x_{AZ',E}}{x_{AZ',A}} \tag{15}$$

It can be stated that the minimum amount of the entrainer decreases if, instead of the heteroazeotrope, the distillate is only withdrawn from the *A*-rich phase.

At finite reflux ratios the possible concentration profiles of the rectifying section must be determined for the specified reflux ratio and overall product composition (x_D^0). Figure 4 shows a rectifying profile map for $R = 10$ when the prescribed distillate composition is Az' [one-phase distillate (point D) is withdrawn from the entrainer–lean phase of the azeotrope].

The node of the rectifying profiles (SN_r) is assigned by the overall reflux composition located between Az and Az'' on the A-E edge, since the given reflux ratio cannot be ensured by returning just the entrainer–rich ($''$) phase of the condensate to the column, and one part of the entrainer–lean phase must also be returned (two-phase reflux). In this case, two liquid phases may appear on several plates of the column. In our case, SN_r is very close to the azeotropic point. In the rectifying profile map a saddle point (S_r) appears (originated from vertex B). There is a new boundary (*rb*) separating the feasible (FR_1, FR_2) and infeasible regions (IR_1, IR_2). This boundary limits the recovery of component A; when the still composition x_S^0 bumps against this boundary, the specified distillate composition (point D) cannot be maintained any longer. In our case, *rb*, which runs further from D than the hlbe, is located in the homogeneous region. The other two separatrices of S_r forming another boundary (*rbu*) separate the two feasible (FR_1 from FR_2) and the two infeasible regions (IFR_1 from IFR_2), respectively.

If only one-phase reflux (of composition Az'') is applied, the specified distillate composition cannot be reached from anywhere and the whole area of the triangle will be infeasible.

On the basis of the analysis of the rectifying profile map, it can be concluded that the following separation steps must be performed in the case of batch addition of the entrainer:

(0) Addition of the whole quantity of E (SF) to the binary charge A-B.

(1) Startup ($R = \infty$).

(2) Production of A (in the Az' composition), two-phase reflux, and one-phase distillate.

(3) Separation of B/E (without decanting).

In the case of continuous feeding of the entrainer, the extractive profile map must be studied. The extractive profile map for a finite reflux ratio is shown in Figure 5.

The stable node of the extractive profiles (SN_e) is located on the A-E edge. Although the stable node is farther from D than in the case of $F/V = 0$ (Figure 4), it remains in the heterogeneous region. Hence, the distillate composition D can be reached on the tie line without a rectifying section. There is a saddle point (S_e, originated from vertex B), and a boundary (*eb*) separates the feasible (FR_1, FR_2) and infeasible regions (IR_1, IR_2). In our case, the extractive boundary limiting the recovery of A is located in the homogeneous region.

On the basis of the analysis of the extractive profile map it can be concluded that the following separation steps must be performed in the case of continuous entrainer feeding:

(0) Addition of a small quantity of E (SF_0) to the binary charge A-B (optional).

(1) Startup ($R = \infty$, $F = 0$).

(2) Production of A (in the Az' composition) under continuous feeding of E ($R < \infty$, $F > 0$; two-phase reflux and one-phase distillate).

(3) Separation of B/E (without decanting).

We can conclude that the separation can be feasible by both batch addition and continuous feeding of E. To compare the maximum recoveries of A, the location of the boundaries of extractive and rectifying profiles must be compared for the given operating conditions.

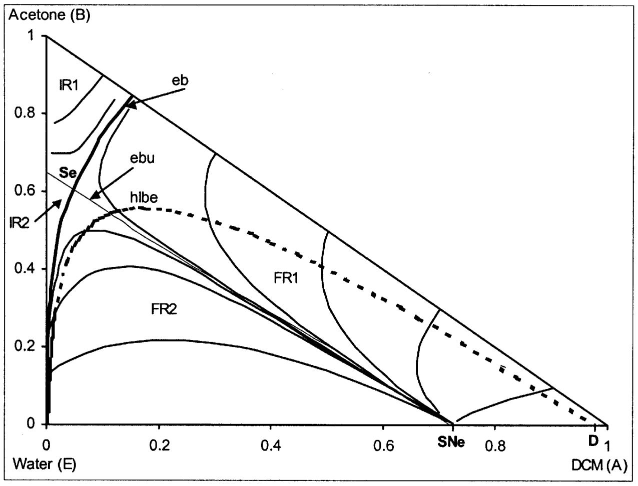

Figure 5. Extractive profile map at a finite reflux ratio ($R = 10$, $F/V = 1/4$ mol/mol).

The stable node of the extractive profiles (SN_e) is located on the A-E edge in the heterogeneous region. The distillate composition D can be reached on the tie line without a rectifying section. The boundary of the extractive profiles (*eb*) limits the recovery of component A.

Before this comparison is made, however, we need to investigate the influence of the operational parameters.

Influence of the Operational Parameters. The influence of the most important operational parameters is investigated for both batch addition and continuous feeding of the entrainer.

(1) Batch Addition of the Entrainer. In this case, the effect of the variation of the reflux ratio and the amount of the entrainer added are studied.

Upon the decrease of the reflux ratio (Figure 6), the rectifying boundary (*rb*) gets closer to the specified distillate composition, so the feasibility region decreases. The node of the rectifying profiles gets further from the azeotropic point according to the change of x_R^0 by the lever rule. This is indicated by the movement of *rbu*.

Below a certain reflux ratio (in our case, $R < 10$), the rectifying boundary enters the heterogeneous region (rb_3). Hence, at the end of Step 2 the still composition belonging to the maximal recovery of A (W^0) may be located on the heterogeneous part of *rb*. The boundary rb_3 does not exhibit any discontinuity or breaking at the heterogeneous liquid boiling envelope, but it passes continuously through it. In the immiscibility gap rb_3 can be crossed by the aid of a tie line. Two liquid phases (W' and W'') can be obtained from the still liquid of composition W^0 by decantation. The concentration of A is higher in W' and in W$''$ is lower than in W^0, respectively. The maximum recovery of A in the distillate is not influenced by the phase separation. In this case, it is also determined by the location of W^0. (However, the loss of A could be obviously reduced by recycling W'.)

There is obviously a minimum reflux ratio (recall the case of one-phase reflux). However, there is no maximum reflux ratio, since the separation is feasible at $R = \infty$.

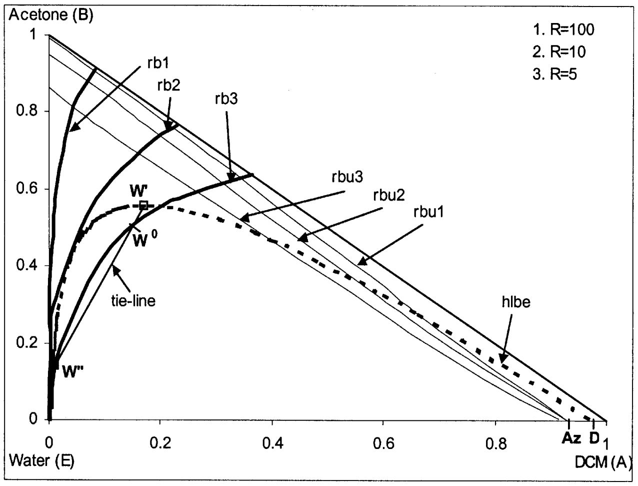

Figure 6. Influence of the reflux ratio on the rectifying boundary.

On the decrease of R, the rectifying boundary *rb* gets closer to the specified distillate composition (point D), so the feasibility region decreases and the rectifying boundary can enter the heterogeneous region. Though in this case the boundary can be crossed by the aid of a tie line, the recovery of A is limited by the location of the boundary *rb*.

If a small quantity of entrainer (SF) is added to the charge, the mixture point (M) remains in the homogeneous region (Figure 7). In this case we have a minimum reflux ratio at which the rectifying boundary passes through the point M (Lang et al., 2000a). By the addition of a greater quantity of entrainer, the mixture point (M^0) can enter the heterogeneous region. In this case, the heterogeneous mixture M^0 can be either directly distilled (the endpoint of the still path is W) or separated into two phases (M', M''), which can be processed separately. In the latter case, a smaller $R_{\min}$ belongs to the $\boldsymbol{E}$-lean phase (M') than to the $\boldsymbol{E}$-rich one (M'').

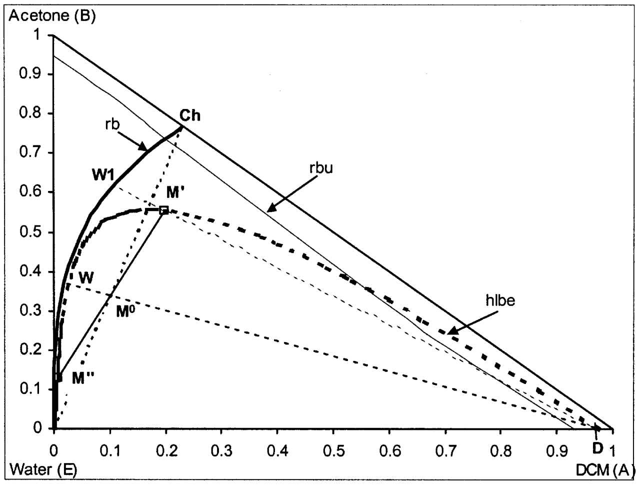

Figure 7. Effect of phase splitting in the case of batch addition of a great quantity of the entrainer.

By the addition of the entrainer the mixture point (M^0) may get into the heterogeneous region. The two liquid phases can be processed separately.

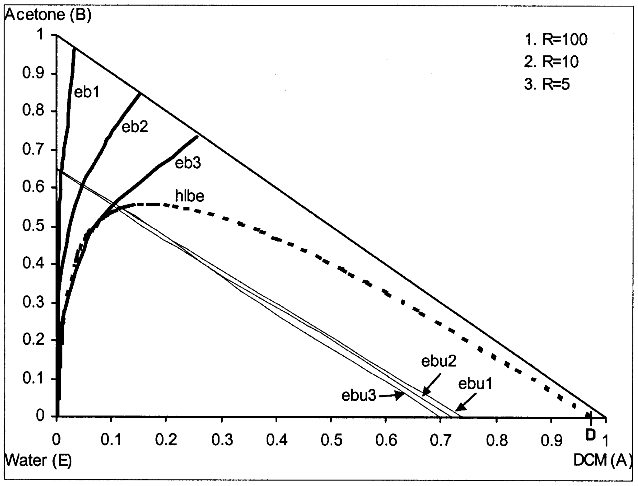

Figure 8. Influence of the reflux ratio on the extractive boundary *eb* ($F/V = 0.25$ mol/mol).

On the decrease of R the extractive boundary *eb* approaches the specified distillate point D, and it can enter the heterogeneous region.

When producing D from the $\boldsymbol{E}$-lean phase (M'), the endpoint of the still path belonging to the maximum recovery of A is W_1. In the E-rich phase the concentration of A is smaller than it was in the charge, and it is doubtful that it is worth producing D from this phase. For a given reflux ratio and charge composition by the increase of the quantity of the entrainer, we can get into the feasible region even if the charge composition is in the infeasible region. On the basis of this fact, a minimum amount of entrainer ($SF_{\min}$) can be determined (Lang et al. 2000a).

(2) Continuous Feeding of the Entrainer. First the case where the entire quantity of the entrainer is fed continuously ($SF_0 = 0$) is considered. The effects of the variation of the reflux ratio under $F/V =$ constant, flow rate of the entrainer (F/V ratio), and reflux ratio under constant entrainer consumption ($SF =$ constant) are studied.

Then the case where, besides the continuous feeding, one part of the entrainer is added in batch to the charge ($SF_0 > 0$) is investigated. For this case, the effects of the variation of the quantity of the entrainer added in batch (SF_0) under $F/V =$ constant, and the ratio of SF_0/SF under constant entrainer consumption ($SF =$ constant) are studied.

On the decrease of R (Figure 8), the extractive boundary (eb) approaches the specified distillate point D, and under a certain value of R, enters the heterogeneous region. (The stable node gets somewhat further from the azeotropic point.)

With the increase in the flow rate of the entrainer (Figure 9), the feasibility region rises, since the extractive boundary recedes from point D. The stable node gets significantly further from the distillate point, as is indicated by the movement of *ebu*. At a higher value of F/V, the stable node can reach the vertex $\boldsymbol{E}$ and can even leave the ternary diagram; there is obviously a maximum F/V ratio.

When the reflux ratio is decreased under constant entrainer consumption (Figure 10), the value of F/V must be simultaneously increased. The extractive boundary (eb) moves as a result of two opposite effects. It would approach point D

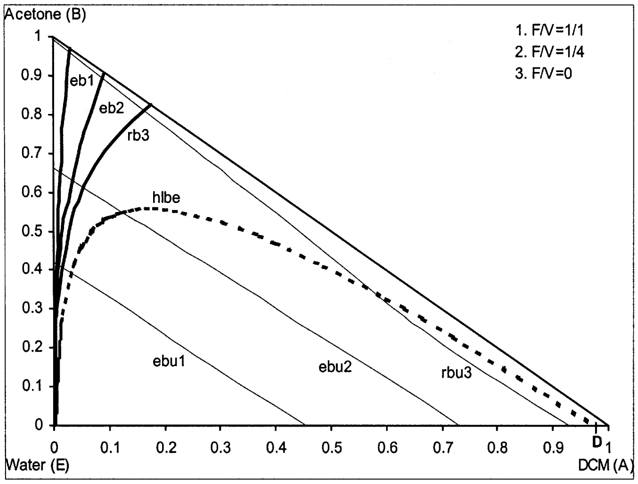

Figure 9. Influence of the *F/V* ratio on the extractive boundary ($R = 20$).

On the increase of the flow rate of the entrainer the extractive boundary (*eb*) removes from point *D* so the feasibility region rises. However, the stable node gets significantly further from the distillate point and it can even leave the ternary diagram.

as a result of the decrease of *R*, and it would get further from *D* due to the increase of *F/V*. In our case, the influence of the decrease of *R* is dominant, so the extractive boundary gets closer to *D* and the feasibility region decreases in the case studied. On the other hand, in the moving of *ebu*, the increase of *F/V* has a major effect, so the stable node gets further from the azeotropic point. This is in agreement with the results obtained for the movement of *eb* and *ebu* by the study of the influence of *R* under $F =$ constant and that of *F/V* under $R =$ constant.

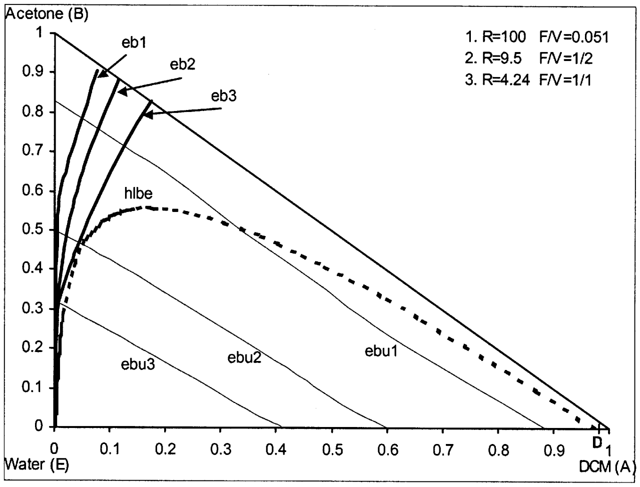

Figure 10. Influence of the variation of *R* on the extractive boundary under $SF =$ constant; on the decrease of *R* and the simultaneous increase of *F*, *eb* got closer to point *D* and *SN* removed from it.

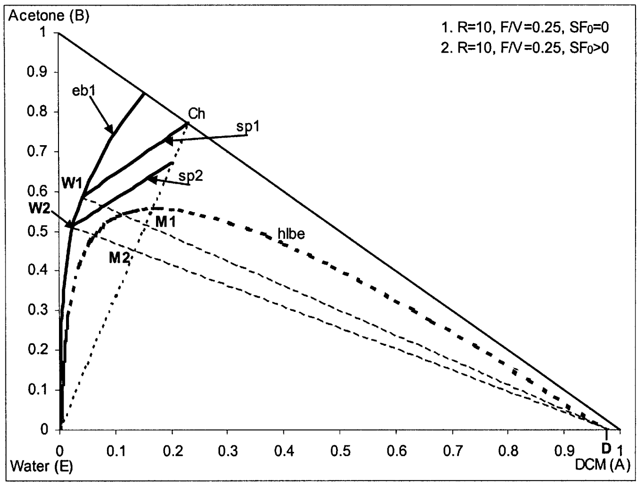

Figure 11. Influence of the variation of the amount of the entrainer added in batch on the still path under $F/V =$ constant ($R = 10$, $F/V = 0.25$ mol/mol, $SF_0 = 0$ and 15 mol).

The modified still path sp_2 is parallel to sp_1. The recovery of *A* rises due to the increased entrainer consumption (M_2 is closer to vertex *E* than M_1).

If besides continuous feeding (*F* is unchanged), some entrainer (SF_0) is added in batch to the charge, the overall quantity of the entrainer applied (*SF*) increases. Hence, the mixture point M_2 gets closer to vertex *E* than M_1 (Figure 11). The location of the extractive boundary does not vary. The modified still path (sp_2), starting from the line $\overline{ECh}$ from the interior of the triangle, is parallel to sp_1. The recovery of *A* rises, that is, $\eta_{A,2} > \eta_{A,1}$. By the application of the lever rule for the batch addition of **E** (mixing) and for the production of *A* (separation of the mixture *M*), the recovery of *A* can be determined by

$$\eta_A = \frac{x_{D,A}}{x_{ch,A}} \frac{\overline{WM}}{\overline{WD}} \frac{\overline{ECh}}{\overline{EM}} \tag{16}$$

that is, η_A is inversely proportional to the length of the line $\overline{EM}$ and proportional to the ratio ($\overline{WM}/\overline{WD}$). In our case, though, the ratio $\overline{WM}/\overline{WD} = SD/(U_{ch} + SF)$ slightly decreased, but the increase in the ratio $\overline{ECh}/\overline{EM} = (U_{ch} + SF)/U_{ch}$ was greater, and so the recovery of *A* increased.

If one part of the entrainer is added in batch under unchanged entrainer consumption ($SF =$ constant), the entrainer flow rate (*F*) must be reduced. Due to the decrease of the ratio *F/V* the modified extractive boundary (eb_2) gets closer to point *D* (Figure 12) and so the feasibility region diminishes. If we try to obtain the same recovery of *A* as in the case of $SF_0 = 0$, the modified still path sp_2 should reach point W_1. On the contrary, when sp_2 arrives at the boundary eb_2 the distillate composition deteriorates ($x_{D,A}$ begins to decrease). If after reaching the boundary we continue the distillation until using up the whole, specified quantity of entrainer (*SF*), the distillate will contain less *A* than prescribed, therefore, $\eta_{A,2}$ will be lower than $\eta_{A,1}$. (This later part of Step 2 cannot be modeled by the feasibility method because of the variation of $\boldsymbol{x}_D$.)

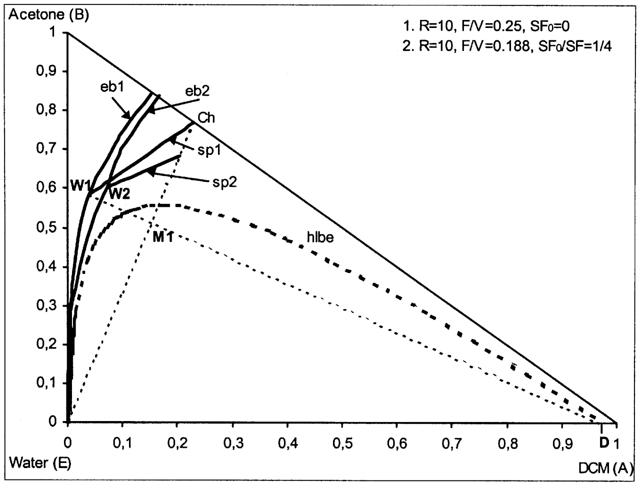

Figure 12. Influence of the variation of the ratio SF_0/SF under SF = constant ($R = 10$, $SF = 50$ mol, $SF_0 = 0$ and 12.5 mol, $F/V = 0.25$ and 0.188 mol/mol).

On the increase of the entrainer addition ratio SF_0/SF because of the simultaneous decrease of F, the extractive boundary *eb* gets closer to point D, and so the feasibility region diminishes.

Comparison of Continuous Feeding and Batch Addition of the Entrainer. Continuous feeding (under $SF_0 = 0$) and batch addition of the entrainer will be compared under constant entrainer consumption (Figure 13).

The extractive boundary (*eb*) is located further from the specified distillate point D—mainly in the region of the moderate entrainer to charge ratios—than the rectifying one (*rb*). The extractive profile (*ep*) crosses the rectifying boundary (*rb*) even at the end of the production step (Step 2). The endpoint of the still path in the case of continuous feeding (W_2) is further from D than in the case of batch addition (W_1). Hence, greater recovery of A can be reached by continuous feeding.

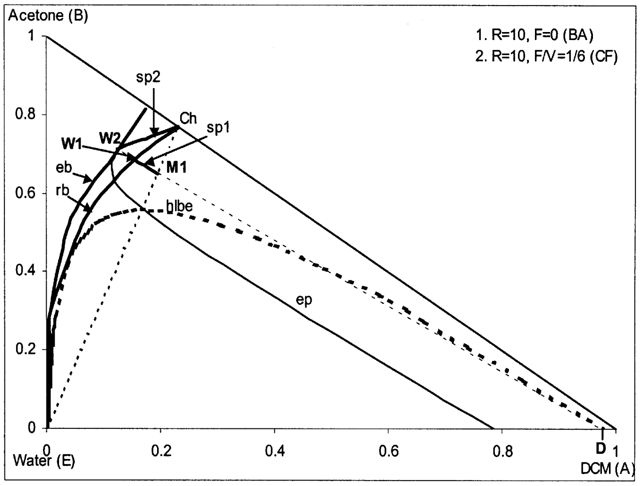

Figure 13. Comparison of the CF and BA of the entrainer under SF = constant.

The extractive boundary is located further from the specified distillate point D mainly in the region of the moderate entrainer to charge ratios than the rectifying one (*rb*).

Rigorous Simulation Results

The feasibility method is based on several simplifying assumptions (such as negligible tray holdup), making the description of the process less accurate. Therefore, the feasibility studies must be completed by rigorous simulation calculations. When making the rigorous simulation, the usual simplifying assumptions were applied:

- Theoretical trays;
- Negligible vapor holdup;
- Constant volume of liquid holdup;
- Negligible fluid dynamic lags.

The model equations to be solved are well-known: (1) nonlinear differential equations (material balances, heat balances); and (2) algebraic equations (VLE, LLE relationships, summation equations, holdup equivalence, physical property models).

For the solution of the preceding equations the CC-BATCH professional simulator (BATCHCOLUMN module of the CHEMCAD 5.0, Chemstations, 2000) was used, applying the simultaneous correction method. The solution method is based on quasi-steady-state approximation.

Example

In the example studied, the aim of the separation is to remove 99% of component $\boldsymbol{A}$ from beside $\boldsymbol{B}$ from the composition charge: $x_{ch,A} = 0.05$, $x_{ch,B} = 0.95$ in Step 2. (In Step 3, $\boldsymbol{B}$ can be easily purified from $\boldsymbol{E}$.) The quantity of the charge is $U_{ch} = 100$ mol ($U_{ch}^{vol} = 7.23$ dm^3). The rectifier contains 22 theoretical plates, including the reboiler (plate 22) and the total condenser with the decanter (plate 1). The volumetric liquid holdup is 50 cm^3/plate, and the heat duty of the reboiler is $Q_N = 1{,}500$ W. Pure entrainer (of boiling point liquid) is used.

Binary Batch Distillation. First conventional batch rectification was simulated without using an entrainer. As was expected on the basis of the binary equilibrium curve (Figure 14), we were not able to remove component $\boldsymbol{A}$ to the prescribed extent from beside $\boldsymbol{B}$, even when we applied a very high ($R = 40$) reflux ratio. [We were able to remove only the 98.1% of $\boldsymbol{A}$ with unacceptably high loss of $\boldsymbol{B}$ (85.8%) before the reboiler dried up].

Even at the end of the startup period under $R = \infty$ the concentration of $\boldsymbol{A}$ was not high enough (35 mol%). In spite of the fact that there is no azeotrope, because of the low relative volatility, high $x_{D,A}$ cannot be reached under the given number of stages and holdup. (Even when the holdup was neglected, a distillate of only 82 mole% was received.)

We concluded that the separation cannot be performed by binary batch distillation due to the unfavorable VLE-conditions, and, therefore, the application of a separating agent is necessary. First we studied the traditional batch addition of the entrainer, and then its continuous feeding.

Batch Heteroazeotropic Distillation (batch addition of the entrainer). Since a simple binary separation was not sufficient, an entrainer was applied to promote the separation. First the startup period under $R = \infty$, then Step 2 were studied.

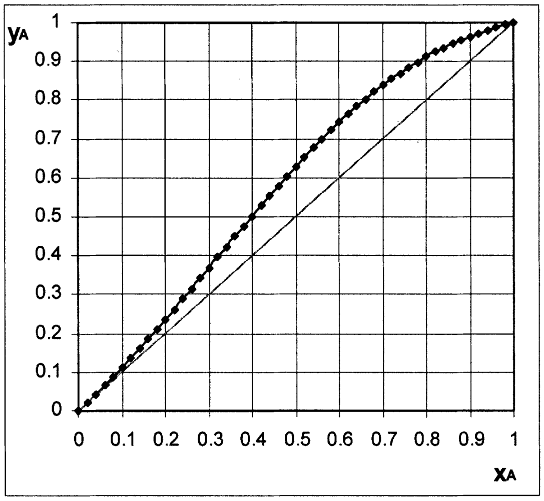

Figure 14. Equilibrium curve of the mixture dichloromethane (*A*)-acetone (*B*); the equilibrium curve is very close to the diagonal mainly at low x_A values.

1. Startup Under $R = \infty$ (Step 1). By adding the entrainer, the volume of the mixture to be distilled increases. [If 200 mol of ***E*** is applied ($SF/U_{ch} = 2.0$ mol/mol), it increases to 10.83 dm^3.] If we supply the condenser with a decanter (with a volume that ensures sufficient residence time for the separation of the condensate), the holdup also rises considerably (such as in the case of a decanter of 150 cm^3 $U_1^{vol} = 200$ cm^3).

With the preceding parameters at the end of Step 1 the condensate is heterogeneous ($\boldsymbol{x}_1^0 = [0.790, 0.168, 0.042]$). However, the concentration of ***B*** is considerable on the plates of the column (such as $\boldsymbol{x}_2 = [0.634, 0.320, 0.046]$) and there is only one liquid phase. The composition of the condensate at the end of Step 1 depends on the quantity of the entrainer and the holdup.

With the increase in the amount of ***E*** (Figure 15, Table 3), the mole fraction of ***A*** and that of ***E*** rise in the condensate.

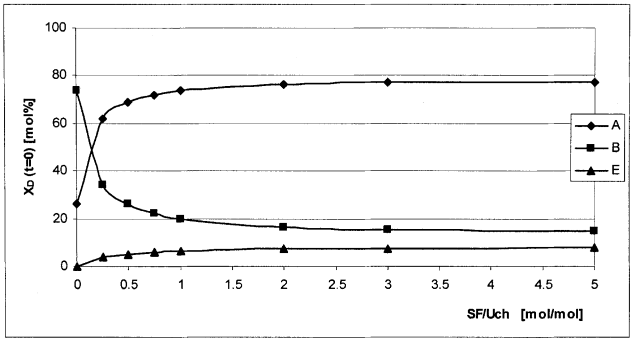

Figure 15. Influence of the quantity of the entrainer added in Step 0 (SF_0) to the condensate composition at the end of Step 1 ($U_1^{vol} = 200$ mL).

On the increase of SF_0, the mole fraction of *A* and that of *E* rises in the condensate. A considerable amount of *E* is necessary to have a heterogeneous condensate at the start of Step 2.

Table 3. Influence of the Quantity of the Entrainer on the Condensate Composition at the End of the Startup Period Under $R = \infty$ (Step 1, $U_1^{vol} = 200$ mL)

SF/U_{ch} (mol/mol)	x_1^0 (mol%) *A*	*B*	*E*	Hetero. plates
0	26.29	73.71	0	—
0.25	62.04	34.15	3.81	—
0.50	68.58	26.30	5.12	—
0.75	71.88	22.19	5.93	1
1.00	73.59	20.00	6.41	1
2.00	76.38	16.27	7.35	1
3.00	77.18	15.18	7.64	1
5.00	77.17	14.79	8.04	1

Under the given conditions we had to apply a large quantity of ***E*** to have heterogeneous condensate at the end of Step 1 ($SF/U_{ch} > 0.5$).

In addition, $\boldsymbol{x}_1^0$ strongly depends on the decanter holdup. With the increase in U_1^{vol}, the mole fraction of ***B*** rises in the condensate to the detriment of those of the two other components (Figure 16, Table 4). The number of the heterogeneous plates decreases and at a certain value ($U_1^{vol} = 250$ mL) the second liquid phase disappears, even in the decanter. (The reason of the strong dependence of $\boldsymbol{x}_1^0$ on the decanter holdup is that the charge contains ***A*** in a low quantity. For higher quantities of ***A*** in the charge, the dependence is less strong.)

According to the preceding results, the minimum amount of entrainer necessary to attain the heterogeneous region with the condensate composition, $\boldsymbol{x}_1^0$, also strongly depends on the holdup. (For example, for $U_1^{vol} = 50$ cm^3, which is already at $SF/U_{ch} = 0.5$, the upper three plates are heterogeneous and $\boldsymbol{x}_1^0 = [0.894, 0.032, 0.074]$).

2. Step 2 with Phase Separation. Step 2 was studied after the startup period. First we tried to remove ***A*** with *one phase reflux* (***E***-rich phase) and *distillate* (***E***-lean phase). In this way, the reflux ratio was extremely low ($R < 0.05$) and the condensate became homogeneous at the beginning of Step 2. This indicates that in our case heterogeneous condensate can only be produced if one part of the ***E***-lean phase is also used as a reflux.

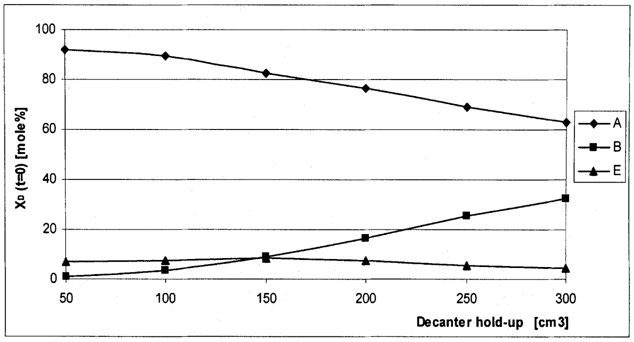

Figure 16. Influence of the decanter holdup on the condensate composition at the end of Step 1 ($SF/U_{ch} = 2.0$ mol/mol).

The increase of the decanter holdup has a negative effect on the condensate purity. If the quantity of *A* is low in the charge, this effect is considerable.

Table 4. Influence of the Decanter Holdup on the Condensate Composition at the End of the Startup Period Under $R = \infty$ (Step 1, SF/U_{ch} = 2.0 mol/mol)

U_1^{vol}		x_1^0 (mol%)		Hetero.
mL	*A*	*B*	*E*	plates
50	92.19	0.92	6.88	1–4
100	89.31	3.27	7.41	1–3
150	82.72	8.82	8.46	1–2
200	76.38	16.27	7.35	1
250	69.04	25.53	5.43	—
300	62.88	32.70	4.41	—

The results obtained with *two-phase reflux* for the different ratios of the ***E***-lean phase withdrawn as distillate (β) are shown in Table 5, where the quantity of the components gained from the decanter (***sd***) during the heterogeneous part of Step 2 can be seen.

Even if a very large part (97.5%) of the ***E***-lean phase is refluxed (Case 3), only a small part (less than 1/3) of ***A*** could be removed while the condensate remained heterogeneous. This means that the decanter is unnecessary in the larger, remaining part of Step 2. Hence, we also investigated the case where the decanter was omitted.

3. Step 2 without Phase-Separation. First we studied the first, shorter part of Step 2 where the condensate is heterogeneous. A reflux ratio that was close to the average reflux ratio of Case 2 ($R = 9$) was applied. The duration of this part was the same as in Case 2.

Without phase separation—letting the decanter holdup unchanged ($U_1^{vol} = 200$ mL)—slightly worse separation was reached than before (***sd*** = [1.43,0.54,0.12 mol]).

When we allowed for the fact that the holdup decreases without the decanter ($U_1^{vol} = 50$ mL), the gain of ***A*** significantly increased, the loss of ***B*** considerably decreased, and the loss of ***E*** rose slightly in comparison with Case 2 (***sd*** = [1.81,0.11,0.16 mol]). Hence, in the first part of Step 2 the separation was significantly better without the decanter due to the diminution of the holdup.

On the basis of the preceding results, further calculations for all of Step 2 were carried out without separating the condensate into two liquid phases. Besides the considerable loss of ***B*** ($\eta_B = 24.9\%$, $\Delta t_2 = 1.60$ h, ***sd*** = [4.95,23.67,0.41 mol]), the prescribed removal of *A* (under $R = 9$) was achieved. The evolution of instantaneous distillate composition $\boldsymbol{x}_D^0$ with the time is shown in Figure 17.

For a very short time (~ 0.15 h) at the beginning of Step 2 the distillate was heterogeneous (Figure 18). At the end of Step 1 ($t = 0$) on four plates two liquid phases occur. Later (at $t = 0.15$ h), only the condensate was heterogeneous. In the remaining part of Step 2 there was only one liquid phase in the whole column ($t = 0.3$ and 1.6 h).

Table 5. Influence of the Refluxed Ratio of the *E*-Lean Phase (1-β) on the Removal of *A* (Batch Addition of *E*)

			sd(mol)		
Case	β	*A*	*B*	*E*	η_A%
1	0.33	1.38	0.48	0.11	27.6
2	0.1	1.46	0.51	0.11	29.2
3	0.025	1.63	0.42	0.10	32.6

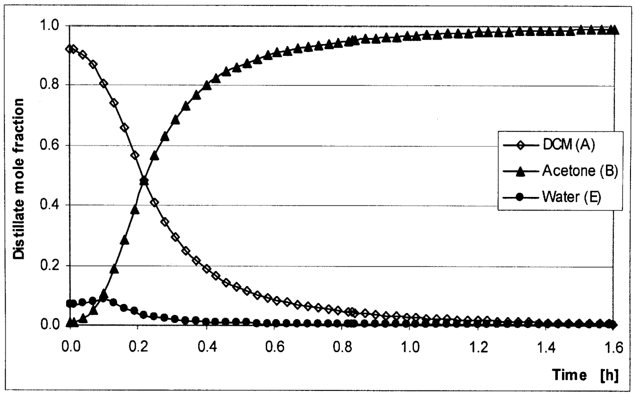

Figure 17. Evolution of the distillate composition x_D^0 with the time (batch addition, SF/U_{ch} = 2 mol/mol, $R = 9$); at the beginning of Step 2 $x_{D,A}^0$ is high for a very short period.

It was found that the prescribed removal of ***A*** can be performed by the batch addition of ***E***, but only at the expense of considerable loss of ***B***. It also can be stated that in the given case, the use of a decanter is not necessary.

Batch Heteroazeotropic Distillation with Continuous Feeding of the Entrainer. On the basis of the favorable results of the feasibility studies, the continuous feeding of the entrainer was also investigated. In the first calculation, the entrainer feeding arrived at the seventh plate with a molar flow rate of 100 mol/h. The decanter was omitted.

The prescribed removal of *A* (under $R = 9$) was achieved again ($\eta_B = 23.4\%$, $\Delta t_2 = 1.51$ h, ***sd*** = [4.95,22.19,1.21 mol]). The evolution of the distillate composition $\boldsymbol{x}_D^0$ with the time is shown in Figure 19. At the end of Step 1 (before the start of the entrainer feeding) the distillate had the same composition as in the case of binary distillation. For a short period ($\Delta t = 0.07$ h) $x_{D,A}$ and $x_{D,E}$ increased. During all of Step 2,

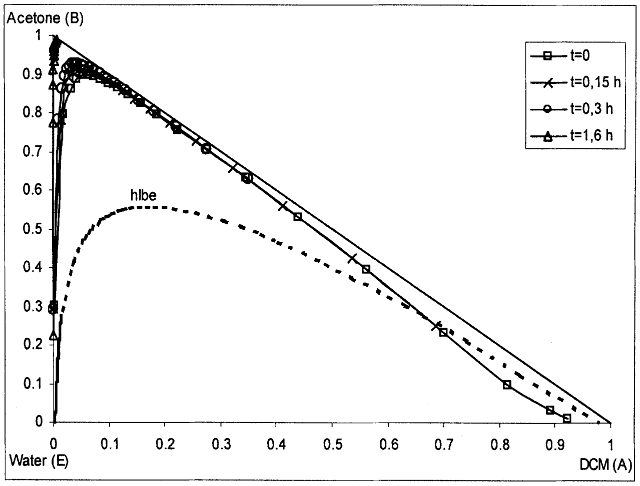

Figure 18. Evolution of the concentration profile in Step 2 (BA; SF/U_{ch} = 2.0 mol/mol, $R = 9$).

At the start of Step 2 the condensate and the liquid phase of the 3 upper plates were heterogeneous. The condensate composition remained in the heterogeneous region for a short period (until $t \approx 0.15$ h).

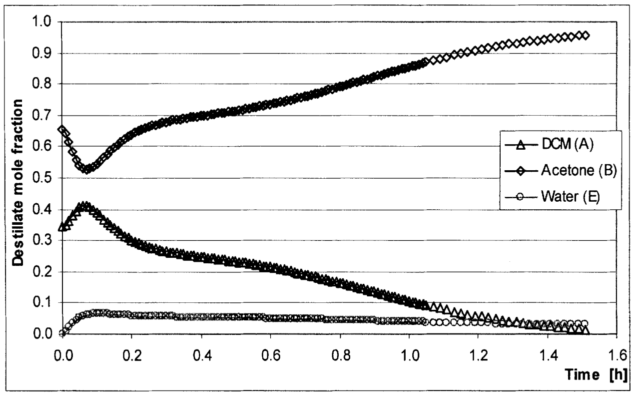

Figure 19. Evolution of the distillate composition x_D^0 with the time (continuous feeding, $F = 100$ mol/h, $R = 9$, $f = 7$); at the start of Step 2 $x_{D,A}$ is low, then it increases for a short period.

the entire concentration profile remained in the homogeneous region (Figure 20). Hence, the uncertainty caused by the presence of two liquid phases on the plates is eliminated. At the beginning of Step 2 ($t = 0$), the concentration profile coincided with that of the binary batch distillation. Later ($t = 0.07$ and 0.75 h) the rectifying and extractive profiles meeting at the entrainer feed plate (plate 7) could be well distinguished. At the end of Step 2 ($t = 1.51$ h) the whole profile was located close to the BE edge.

It was found that the prescribed removal of *A* also can be performed by continuous feeding of ***E***, and that the continuous feeding may be oppositional to the traditional batch addition. Before comparing the batch addition and the continuous feeding of the entrainer, the influence of the most important operational parameters was investigated for both methods.

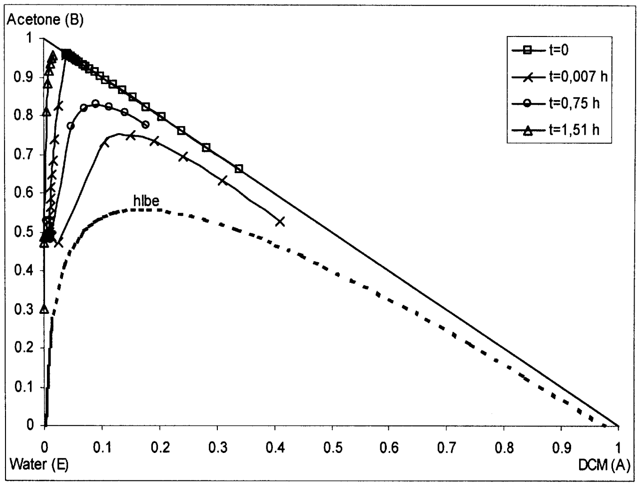

Figure 20. Evolution of the concentration profile in the case of continuous feeding of the entrainer; during the entire Step 2 the whole column profile remained in the homogeneous region.

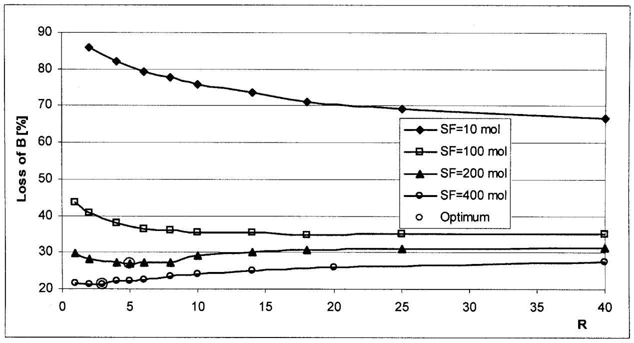

Figure 21. Influence of the reflux ratio on the relative loss of *B* (BA; SF/U_{ch} = 0.1, 1.0, 2.0, 4.0 mol /mol); at higher solvent to charge ratios, there is an optimum reflux ratio where the loss of *B* is minimal.

Influence of the operational parameters

The influence of the most important operational parameters was investigated for both batch addition and continuous feeding of the entrainer. The following input data were always kept constant: $N = 22$, $Q_{N+1} = 1{,}500$ W, and $U_j^{\mathrm{vol}} = 50$ cm^3/plate ($j = 1, \ldots, N-1$).

Batch Addition of the Entrainer. In this case, the entire quantity of ***E*** was added to the charge at once, and there was no continuous feeding ($F/V = 0$). We studied the effect of the variation of

- The reflux ratio, and
- The amount of the entrainer added.

Step 2 was finished when, for the instantaneous distillate composition the following criterion was satisfied: $x_{D,A} \leq 0.005$.

The influence of the variation of *R* was studied for four different amounts of entrainer ($SF = 10$, 100, 200, and 400 mol). With the increase in the reflux ratio, the distillate withdrawal rate, *D*, decreased, the length of Step 2 (Δt_2) and, proportionally to Δt_2, the energy consumption (SQ) increased. The variation in the relative loss of ***B*** (η_B) is shown in Figure 21.

When a very small amount of ***E*** was applied ($SF/U_{ch} = 0.1$), though on the increase of *R*, the loss of ***B*** decreased in a monotone way, the loss of ***B*** remained very large, even if *R* was very high. For a higher quantity of ***E*** ($SF/U_{ch} = 1.0$), first the loss significantly decreased, then it hardly changed. For an even higher quantity of ***E*** ($SF/U_{ch} = 2.0$), there was an optimum reflux ratio ($R_{\mathrm{opt}} = 5$) where η_B had a minimal value. Above R_{opt} the increase in *R* had a detrimental effect. With a further increase in the quantity of ***E*** ($SF/U_{ch} = 4.0$), the value of R_{opt} became lower ($R_{\mathrm{opt}} = 3$).

Both $x_{D,E,av}$ and the loss of entrainer (sd_E) decreased in a monotone way with increasing *R* for each SF/U_{ch} ratio. For the higher SF/U_{ch} values, $x_{D,A,av}$ had a maximum at R_{opt} (Table 6).

The influence of the amount of the entrainer (SF) was investigated under three different reflux ratios ($R = 1,4,10$). By increasing SF, the removal of *A* became more efficient ($x_{D,A,av}$ increased); the duration of Step 2 and the amount of the distillate (SD) decreased in a monotone way in each case

Table 6. Influence of the Variation of the Reflux Ratio (BA; $SF/U_{ch} = 2.0$ mol/mol)

R	$x_{D,av}$ A	B	E	SD (mol)	Loss of B (%)	Δt_2 (h)
1	0.1456	0.8256	0.0287	34.11	29.6	0.38
2	0.1530	0.8256	0.0214	32.47	28.2	0.54
4	0.1578	0.8256	0.0166	31.49	27.4	0.87
5	0.1597	0.8247	0.0156	31.09	27.0	1.03
6	0.1586	0.8267	0.0147	31.32	27.3	1.21
8	0.1589	0.8273	0.0137	31.23	27.2	1.55
10	0.1505	0.8370	0.0125	32.98	29.1	2.00
14	0.1464	0.8421	0.0115	33.88	30.0	2.80
18	0.1442	0.8449	0.0109	34.40	30.6	3.60
25	0.1420	0.8477	0.0103	34.93	31.2	5.00
40	0.1416	0.8486	0.0098	35.00	31.3	7.90

Table 7. Influence of the Variation of the Amount of the Entrainer (BA; $R = 4$)

SF (mol)	$x_{D,av}$ A	B	E	SD (mol)	Loss of B (%)	Δt_2 (h)
50	0.0893	0.8983	0.0124	55.55	52.5	1.53
100	0.1189	0.8674	0.0137	41.72	38.1	1.15
150	0.1426	0.8419	0.0155	34.81	30.8	0.96
200	0.1589	0.8244	0.0166	31.27	27.1	0.86
250	0.1700	0.8125	0.0175	29.25	25.0	0.81
400	0.1882	0.7930	0.0188	26.43	22.1	0.74
500	0.1951	0.7855	0.0194	25.51	21.1	0.72

(Table 7). The loss of ***B*** also fell, but less and less sharply (Figure 22). The $\eta_B - SF$ curve was steepest for the lowest R ($R = 1$) and was least steep for the highest one ($R = 10$). For the smallest amount of E ($SF = 50$ mol), the best separation was achieved with the highest R, while for the greatest amount of E, the lowest R provided the best separation. However, for the medium SF values, there was a region where the medium R ($R = 4$) gave the best separation. Although by increasing SF the E-content of the distillate ($x_{D,E,av}$) increased, the loss of ***E*** decreased due to the considerable decrease in SD.

Continuous Feeding of the Entrainer. First the entire quantity of ***E*** was introduced to the column continuously ($SF_0/SF = 0$). We studied the effect of the variation of the

- Reflux ratio under constant entrainer flow rate ($F =$ const.);
- Flow rate of the entrainer;
- Entrainer feed plate (f).

In the preceding cases, Step 2 was finished by the criterion used for the batch addition. In these cases the entrainer consumption is not kept constant, since the duration of Step 2 changes. Therefore, we also investigated the influence of the variation of

- R under constant entrainer consumption and a constant amount of distillate ($SF =$ const., $SD =$ const.)
- R under constant entrainer and energy consumptions ($SF =$ const., $SD =$ const.)

The influence of the reflux ratio under $F =$ const. was investigated for three different flow rates of E ($F = 10{,}100{,}250$ mol/h). By increasing R, the duration of Step 2 rose (Table 8). Hence, the consumption of both the entrainer and energy increased. The separation improved, the A-content of the distillate ($x_{D,A,av}$) increased, and the loss of ***B*** (η_B) fell monotonously (Figure 23). $x_{D,E,av}$ varied in a narrow range (it had a minimum in each case). However, the loss of ***E*** diminished monotonously due to the decrease in SD.

The influence of the feed flow rate of the entrainer was investigated for three different reflux ratios ($R = 4$, 10, 20). When increasing the value of F, the separation ***A/B*** became more efficient (Table 9). The stopping criterion was fulfilled

Table 8. Influence of the Variation of the Reflux Ratio Under $F =$ Constant (CF; $F = 100$ mol/h)

R	$x_{D,av}$ A	B	E	SD (mol)	Loss of B (%)	Δt_2 (h)
1	0.0657	0.8637	0.0706	75.85	69.0	0.82
2	0.0803	0.8624	0.0573	62.07	56.3	1.00
4	0.1054	0.8436	0.0510	47.30	42.0	1.26
6	0.1273	0.8226	0.0501	39.16	33.9	1.46
8	0.1479	0.8015	0.0506	33.73	28.5	1.62
10	0.1645	0.7841	0.0514	30.33	25.0	1.78
14	0.1957	0.7506	0.0537	25.49	20.1	2.04
18	0.2182	0.7263	0.0555	22.87	17.5	2.32
25	0.2512	0.6901	0.0587	19.85	14.4	2.76
40	0.2794	0.6602	0.0604	17.86	12.4	3.92

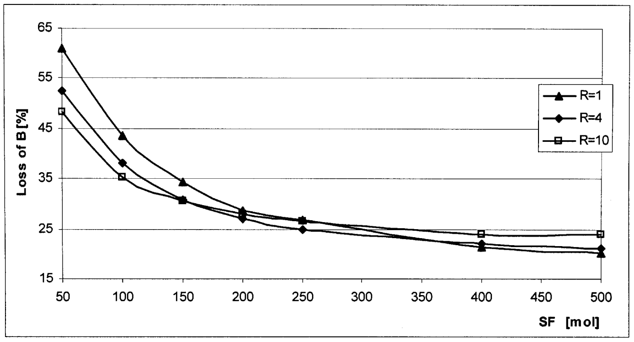

Figure 22. Influence of the amount of entrainer on the relative loss of *B* (BA; *R* = 1, 4, 10).

On the increase of *SF*, the loss of ***B*** decreased in a monotone way in each case. The extent of the decrease depends on the reflux ratio.

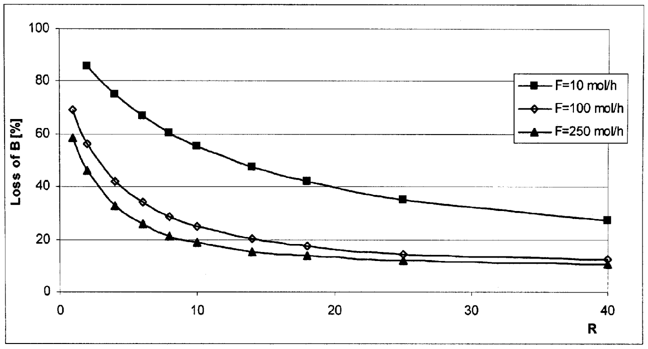

Figure 23. Influence of the reflux ratio on the relative loss of *B* under *F* = constant (CF; *F* = 10, 100, 250 mol/h); on the raise of *R* Δt_2, *SF* and *SQ* increase and the loss of *B* falls.

Table 9. Influence of the Variation of the Feed Flow Rate of the Entrainer (CF; $R = 10$)

F (mol/h)	$x_{D,av}$ A	B	E	SD (mol)	Loss of B (%)	Δt_2 (h)
10	0.0838	0.8832	0.0330	59.40	55.2	3.62
25	0.1079	0.8509	0.0412	46.15	41.3	2.80
50	0.1336	0.8197	0.0467	37.31	32.2	2.24
75	0.1510	0.7994	0.0496	33.03	27.8	1.94
100	0.1645	0.7841	0.0514	30.33	25.0	1.78
150	0.1836	0.7625	0.0539	27.17	21.8	1.56
200	0.1975	0.7470	0.0555	25.27	19.9	1.42
250	0.2052	0.7382	0.0566	24.31	18.9	1.34

Table 10. Influence of the Feed-Stage Location (CF; $F = 100$ mol/h, $R = 10$)

f	$x_{D,av}$ A	B	E	SD (mol)	Loss of B (%)	Δt_2 (h)
2	0.1708	0.6742	0.1550	29.23	20.7	1.80
4	0.1647	0.7567	0.0786	30.29	24.1	1.80
6	0.1583	0.7908	0.0509	31.51	26.2	1.85
8	0.1531	0.8106	0.0363	32.56	27.8	1.90
10	0.1448	0.8282	0.0270	34.41	30.0	2.00
14	0.1341	0.8498	0.0161	37.14	33.2	2.15

earlier (Δt_2 and SD decreased) in each case. The loss of ***B*** monotonously diminished (Figure 24). Although the entrainer content of the distillate ($x_{D,E,av}$) increased, the loss of ***E*** (sd_E) decreased due to the reduction in the amount of distillate.

In the case of continuous feeding of ***E***, the feed stage location provided an additional degree of freedom compared with the batch addition. The influence of the feed-stage location was investigated for three different reflux ratios ($R = 4$, 10, 20 at $F = 100$ mol/h) and for three different entrainer flow rates ($F = 50$, 100, 250 mol/h at $R = 10$).

The increase in the length of the rectifying section to the detriment of the extractive section had a negative influence on the separation ***A/B*** and a positive effect on the separation ***A/E***, respectively. Hence, $x_{D,B,av}$ increased, and $x_{D,E,av}$ diminished considerably (Table 10). The A-content of the distillate ($x_{D,A,av}$) decreased, so the duration of Step 2 (and the amount of the distillate) rose slightly. The loss of ***B*** significantly increased (Figure 25), while the loss of ***E*** diminished. In each case, the optimum feed stage was the top plate of the column ($f_{\text{opt}} = 2$).

So far when investigating the influence of the reflux ratio, the entrainer consumption (SF) did not stay constant. The effects of the variation of R were also studied under $SF =$ const. First, besides SF, the quantity of the distillate remained unchanged ($SD =$ const.). With the increase in R, the time necessary for obtaining the same quantity of distillate increased since

$$\Delta t_{2,\text{new}} = SD \cdot (R_{\text{new}} + 1)/V_2 \tag{17}$$

where V_2 is the vapor molar flow rate arriving at the condenser.

The energy consumption increased proportionally to Δt_2, since $SQ = Q \cdot \Delta t_2$ and Q was unchanged. Since the heat balances were taken into consideration, V_2 varied slightly when changing R. Therefore, we had to ensure the simultaneous constancy of SF and SD in an iterative manner. First, the

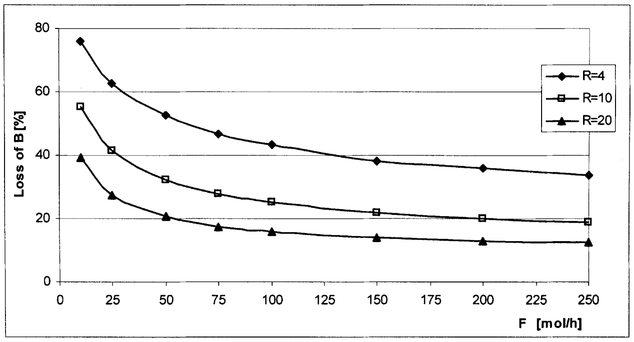

Figure 24. Influence of the feed flow rate of the entrainer on the relative loss of *B* (CF; *R* = 4, 10, 20); with increasing the entrainer feed rate, Δt_2 and *SD* decrease and the loss of *B* diminishes in a monotone way.

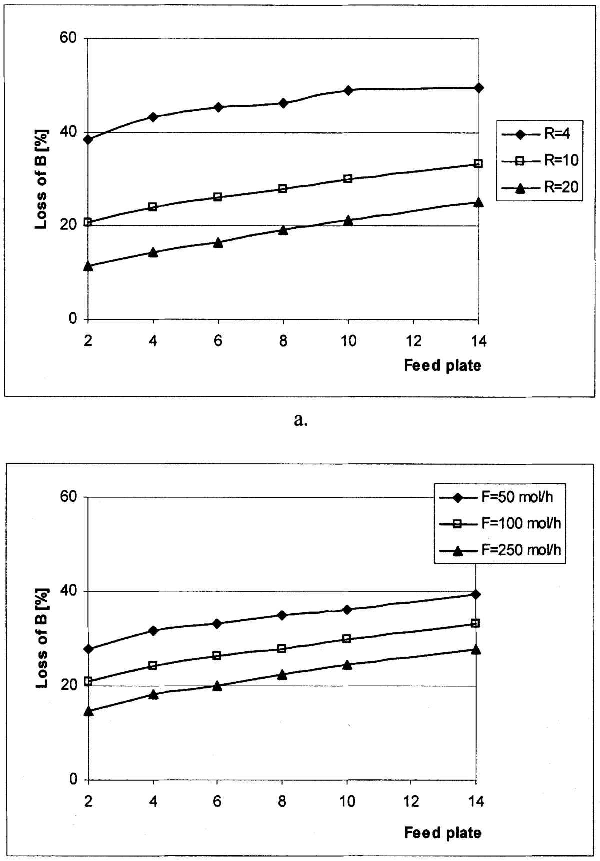

a.

b.

Figure 25. Influence of feed-stage location on the relative loss of *B* (CF; (a) *F* = 100 mol/h, *R* = 4, 10, 20; (b) *R* = 10, *F* = 50, 100, 250 mol/h); the optimum feed stage is the top plate of the column ($f_{\text{opt}} = 2$).

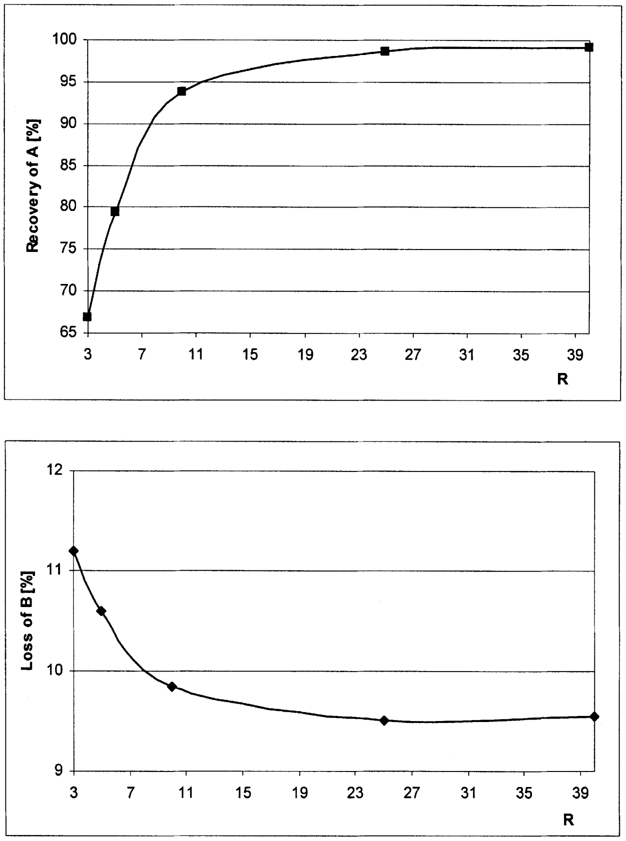

Figure 26. Influence of the variation of the reflux ratio under constant entrainer consumption and amount of distillate on the recovery of *A* and the relative loss of *B* (CF; $SF = 205$ mol, $SD = 15$ mol); on the increase of the reflux ratio, the recovery of *A* increases and the loss of *B* decreases in a monotone way.

new value of F was calculated by the assumption of unchanged V_2 by

$$F_{\text{new}} = F \cdot (R+1)/(R_{\text{new}}+1) \tag{18}$$

and we determined the time ($\Delta t_{2,\text{corr}}$) necessary for obtaining a quantity of distillate SD by the first simulation calculation. Then for the second simulation calculation, F_{new} was corrected so that the $SF = \text{const.}$ condition could be satisfied ($F_{\text{new,corr}} = SF/\Delta t_{2,\text{corr}}$). In the majority of the cases, Δt_2 did not change more, and so one correction of F_{new} was enough. The results are shown in Figure 26.

On the increase of R under constant SF and SD, the recovery of A (proportional to $x_{D,A,av}$; Table 11) increased and the loss of B decreased monotonously (there was no optimum reflux ratio). The loss of E remained almost constant.

Finally, the influence of the reflux ratio was investigated under the simultaneous constancy of the entrainer and heat consumption by keeping the duration of Step 2 constant ($\Delta t_2 = 1$ h, $F = 10$, 100, 250 mol/h). In this case, with the raise of R the amount of distillate decreased by Eq. 17.

With the increase in the reflux ratio, the concentration of A in the distillate ($x_{D,A,av}$) increased, while that of B decreased (Table 12). The entrainer concentration of the distillate ($x_{D,E,av}$) varied in a relatively narrow region, but it had a minimum in each case. Both η_A and η_B monotonously diminished (Figure 27). The extent of the decrease of η_B got smaller and smaller ($|d\eta_B/dR|$ diminished). The entrainer flow rate had a slight influence on the η_B-R curves. However, it had a very significant effect on the η_A-R curves. At the highest value

Table 11. Effects of the Variation of the Reflux Ratio Under Constant Entrainer Consumption and Amount of Distillate (CF; $SF = 205$ mol; $SD = 15$ mol)

	F	$x_{D,av}$			Recovery	Loss of	Δt_2
R	(mol/h)	A	B	E	of A (%)	B (%)	(h)
3	820.00	0.2228	0.7099	0.0673	66.8	11.2	0.24
5	500.00	0.2644	0.6709	0.0647	79.3	10.6	0.40
10	250.00	0.3120	0.6216	0.0664	93.8	9.8	0.82
25	98.56	0.3297	0.6036	0.0667	98.6	9.5	2.09
40	61.38	0.3302	0.6039	0.0660	99.1	9.5	3.35

Table 12. Influence of the Variation of the Reflux Ratio Under Constant Entrainer and Heat Consumption (CF; $\Delta t_2 = 1$ h; $F = 100$ mol/h)

	$x_{D,av}$			SD	Recovery	Loss of
R	A	B	E	(mol)	of A (%)	B (%)
1	0.0545	0.8747	0.0708	91.68	99.8	84.4
2	0.0800	0.8623	0.0576	62.07	99.4	56.3
4	0.1283	0.8185	0.0532	37.38	95.8	32.2
6	0.1735	0.7719	0.0545	26.75	92.8	21.7
8	0.2169	0.7258	0.0573	20.81	90.2	15.9
10	0.2587	0.6806	0.0607	17.03	88.2	12.2
14	0.3378	0.5944	0.0678	12.48	84.2	7.8
18	0.4105	0.5145	0.0750	9.84	80.8	5.3
25	0.5204	0.3930	0.0866	7.16	74.6	3.0
40	0.6773	0.2238	0.0989	4.53	61.4	1.1

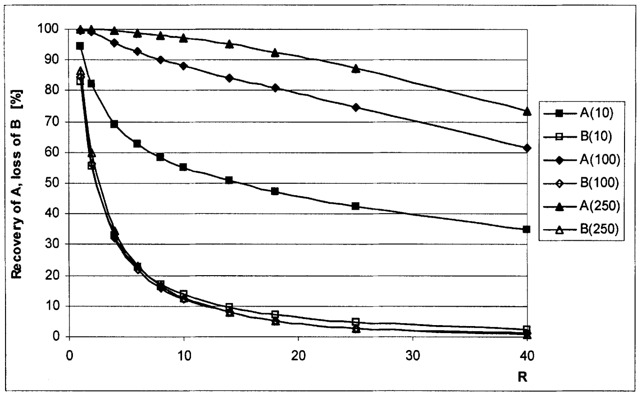

Figure 27. Influence of the reflux ratio on the recovery of *A* and the relative loss of *B* under constant entrainer and heat consumption (CF; $\Delta t_2 = 1$ h; $F = 10$, 100, 250 mol/h).

With the raise of the reflux ratio, the amount of distillate decreases and both the recovery of A and the loss of B monotonously decrease. At the highest value of F, the recovery of A remained high in the large region of R, while the loss of B decreased very quickly in this region.

of F ($F = 250$ mol/h), η_A remained high in a large region (between $R = 1$ and $R = 10$) while η_B decreased considerably in this region. This fact suggests that there is an optimum reflux ratio (R_{opt}), where η_A is still high and η_B is already low.

Mixed Addition of the Entrainer. So far when making rigorous calculations the total quantity of the entrainer was introduced continuously to the column ($SF_0/SF = 0$). In this case Step 2 began with a distillate of a relatively low A-content. On the other hand, the batch addition of the entrainer provided much higher $x_{D,A}$ at the beginning of Step 2. Therefore, the combination of the batch addition and continuous feeding of the entrainer (mixed addition) was investigated. We added one part of $\boldsymbol{E}$ to the charge in Step 0 (SF_0) and the other part continuously during Step 2 (SF_2). We studied the influence of the variation of the increased entrainer ratio SF_0/SF under constant entrainer and energy consumption. The duration of Step 2 was was kept constant ($\Delta t_2 = 1$ h). This study was performed for two different entrainer to charge ratios ($SF/U_{ch} = 1$ and 2, respectively).

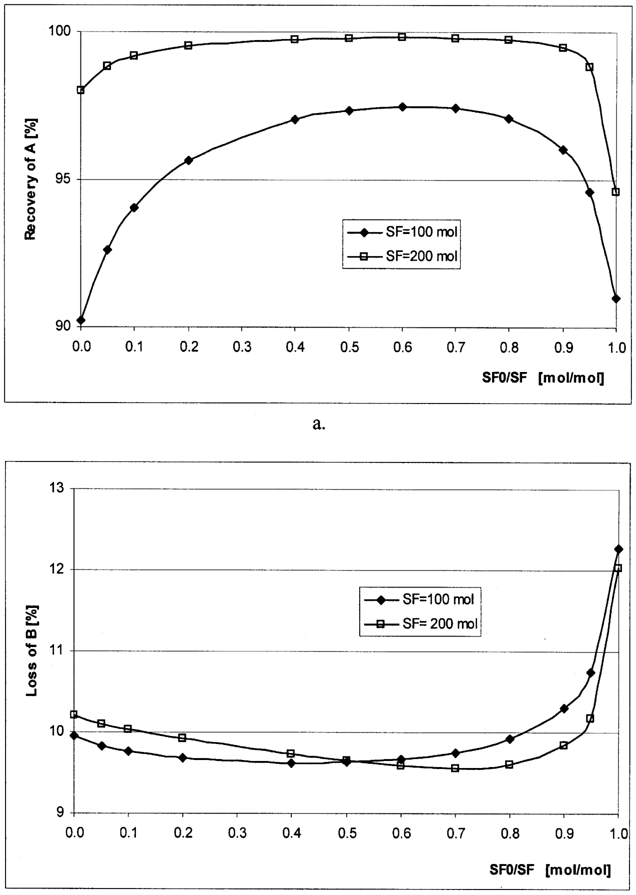

a.

b.

Figure 28. (a) Influence of SF_0/SF on the recovery of A, and (b) the relative loss of B under constant entrainer and heat consumption (mixed addition; $f = 2$, $\Delta t_2 = 1$ h; $R = 10$, $SF = 100$ and 200 mol).

At the medium values of SF_0/SF, both the recovery of A and the loss of $\boldsymbol{B}$ were significantly more favorable than at the low and high values of SF_0/SF.

Table 13. Effects of the Variation of the Ratio SF_0/SF Under Constant Entrainer and Heat Consumption (Mixed Addition; $f = 2$; $\Delta t_2 = 1$ h; $R = 10$, $SF = 200$ mol)

	sd (mol)			Recovery	Loss of
SF/SF_0	A	B	E	of A (%)	B (%)
0	4.90	9.70	2.52	98.0	10.2
0.05	4.94	9.59	2.51	98.8	10.1
0.1	4.96	9.53	2.49	99.2	10.0
0.2	4.98	9.43	2.45	99.5	9.9
0.4	4.99	9.25	2.35	99.8	9.7
0.5	4.99	9.17	2.30	99.8	9.7
0.6	4.99	9.11	2.22	99.8	9.6
0.7	4.99	9.09	2.12	99.8	9.6
0.8	4.99	9.13	1.99	99.7	9.6
0.9	4.97	9.34	1.74	99.5	9.8
0.95	4.94	9.67	1.49	98.8	10.2
1	4.73	11.43	0.37	94.6	12.0

In both cases for both values of SF the recovery of $\boldsymbol{A}$ had a maximum (at $SF_0/SF = 0.6$, Figure 28) and the loss of $\boldsymbol{B}$ had a minimum (for $SF = 100$ at $SF_0/SF = 0.4$, and for $SF = 200$ at $SF_0/SF = 0.7$). The loss of $\boldsymbol{E}$ diminished in a monotone way as the SF_0/SF ratio increased (Table 13). In both cases at the medium values of SF_0/SF (such as at $SF_0/SF = 0.5$), both the recovery of $\boldsymbol{A}$ and the loss of $\boldsymbol{B}$ were significantly more favorable than at very low (such as $SF_0/SF = 0.05$) and very high (such as $SF_0/SF = 0.95$) values of SF_0/SF. These results suggest that there must be an optimum SF_0/SF ratio (where η_A is high and simultaneously η_B is low).

The evolution of the distillate composition for the mixed addition (for $SF_0/SF = 0.5$) is shown in Figure 29. Step 2 begins with a high distillate concentration of $\boldsymbol{A}$, similar to the batch addition, but in this case, $x_{D,A}$ remains high for a longer period.

Comparison of the different entrainer addition methods

We compared the traditional batch, the newly proposed mixed addition (with $SF_0/SF = 0.5$), and the continuous feed-

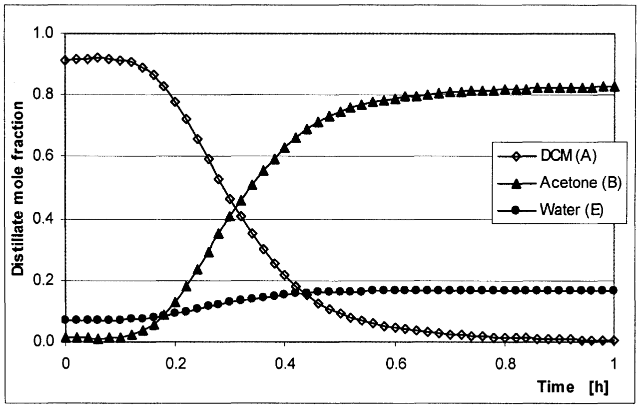

Figure 29. Evolution of the distillate composition in the case of the mixed addition of the entrainer ($f = 2$, $\Delta t_2 = 1$ h; $R = 10$; $SF = 200$ mol; $SF_0/SF = 0.5$).

Due to the effect the entrainer added in Step $0 x_D^0$ is near to the azeotropic composition at the start of Step 2. Similarly to the BA, in this case $x_{D,A}$ remains high for a longer period.

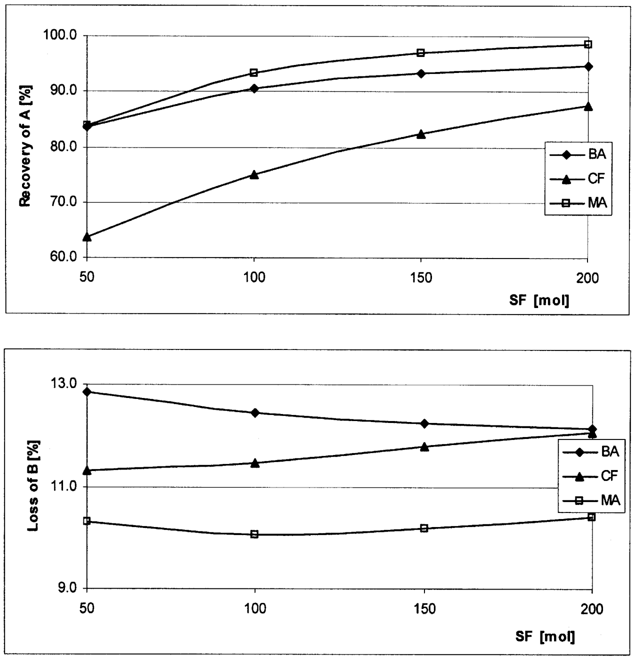

Figure 30. Comparison of the different entrainer addition methods under constant entrainer and heat consumption ($R = 4$; $f = 2$; $\Delta t_2 = 28$ min); for each entrainer consumption, the mixed addition gave the highest recovery of *A* and the lowest relative loss of *B*.

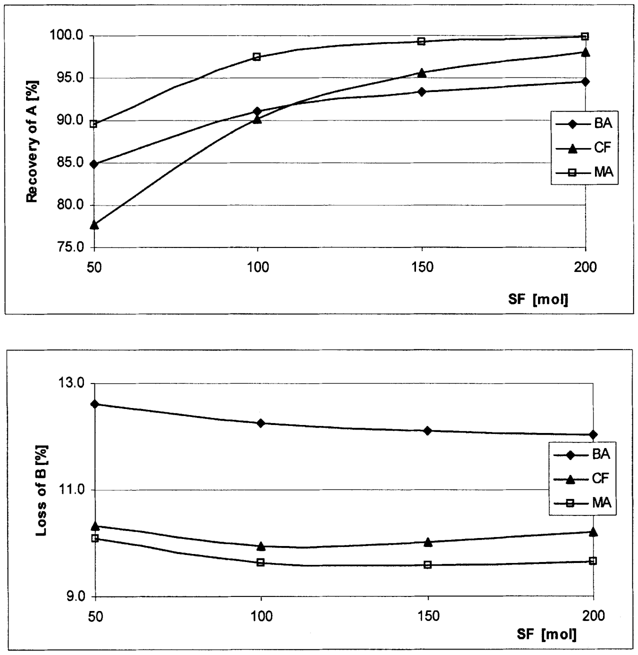

Figure 31. Comparison of different entrainer addition methods under constant entrainer and heat consumption ($R = 10$; $f = 2$; $\Delta t_2 = 1$ h); for each entrainer consumption, the mixed addition gave the highest recovery of *A* and the lowest relative loss of *B*.

ing of the entrainer under constant entrainer and heat consumption for four different entrainer quantities ($SF/U_{ch} = 0.5$, 1, 1.5, 2) and two different reflux ratios ($R = 4$ and 10). The duration of Step 2 was fixed (for $R = 4$, $\Delta t_2 = 0.467$ h and for $R = 10$, $\Delta t_2 = 1$ h).

The best separation (highest recovery of *A*, lowest loss of ***B***) was obtained by the mixed addition in all eight cases (Figures 30 and 31, Table 14). The continuous feeding was competitive with batch addition. It resulted in a lower loss of ***B*** in all the eight cases than the batch addition. Regarding the recovery of *A* for the higher reflux ratio ($R = 10$), it provided higher values for the higher entrainer quantities ($SF/U_{ch} > 1$). For the lower reflux ratio ($R = 4$), continuous feeding yielded a lower recovery of *A* for the entire region of SF/U_{ch} studied.

The proper optimization of the different entrainer addition methods exceeds the limits of this article. The comparison of these methods for two additional mixtures will be presented elsewhere (Modla et al., 2003; Lang et al., 2003).

Conclusion

The separation of a low-relative-volatility, zeotropic mixture in a batch rectifier with the aid of a heavy entrainer forming a binary heteroazeotrope with one of the components was studied first by feasibility studies, then by rigorous simulation. The calculations were performed for the mixture dichloromethane(***A***)–acetone(***B***) by using water as a heterogeneous entrainer (***E***). The possibility of continually feeding the entrainer besides its usual batch addition was also studied.

The method of Lelkes et al. (1998b) was extended for the assessment of the feasibility of the heteroazeotropic distillation in a batch rectifier. The method is based on the analysis of the map of the possible overall liquid composition profiles

Table 14. Comparison of Different Entrainer Addition Methods Under Constant Entrainer and Heat Consumption [$R = 10$; $f = 2$; $\Delta t_2 = 1$ h; (a) BA; (b) CF; (c) MA ($SF_0/SF = 0.5$)]

SF (mol)	***sd*** (mol) *A*	*B*	*E*	Recovery of *A* (%)	Loss of *B* (%)
(a) Batch addition					
50	4.24	11.99	0.31	84.8	12.6
100	4.55	11.65	0.35	91.0	12.3
150	4.67	11.50	0.37	93.4	12.1
200	4.73	11.43	0.37	94.6	12.0
(b) Continuous feeding					
50	3.89	9.80	2.30	77.8	10.3
100	4.51	9.45	2.39	90.2	9.9
150	4.78	9.52	2.45	95.6	10.0
200	4.90	9.70	2.52	98.0	10.2
(c) Mixed addition ($SF_0/SF = 0.5$)					
50	4.48	9.59	1.93	89.6	10.1
100	4.87	9.15	2.11	97.4	9.6
150	4.96	9.11	2.21	99.2	9.6
200	4.99	9.17	2.29	99.8	9.7

of the column sections. The map also contains the heterogeneous liquid boiling envelope with the tie lines. The separation steps and the limiting values of the operational parameters (minimum reflux ratio, maximum flow rate of $\boldsymbol{E}$) were determined for both the batch addition and the continuous feeding of the entrainer. After studying the step where $\boldsymbol{A}$ is withdrawn by the aid of $\boldsymbol{E}$ (Step 2), it can be stated that the separation is feasible even without a rectifying section. It was found that by the continuous feeding, a significantly greater recovery of $\boldsymbol{A}$ can be obtained at a moderate entrainer-to-charge ratio under the same entrainer and energy consumption than by the traditional batch addition.

After the feasibility studies, rigorous simulation calculations were carried out by the CCBATCH professional simulator. Contrary to the feasibility calculations, the liquid holdup was taken into consideration and the number of theoretical plates was fixed. The purification of $\boldsymbol{B}$ from a small amount of $\boldsymbol{A}$ was investigated.

We stated that a two-phase reflux must be applied and that the separation of the top condensate by decantation is not necessary, since in this case the benefits of the phase separation are lost by the increase in holdup caused by the decanter.

The continuous feeding provides additional degrees of freedom (such as entrainer feed stage (f)). By continuous feeding, the column profile could be kept in the homogeneous region from the beginning to the end of Step 2. The influence of the most important parameters was also studied for both batch addition and continuous feeding. The optimum value of the operational parameters was also determined (such as R_{opt}, f_{opt}).

We also investigated the combination of batch addition and continuous feeding (mixed addition) of the entrainer by adding one part of the entrainer to the charge in Step 0 (SF_0) in batch and the other part continuously during Step 2 (SF_2). Comparing the different entrainer addition methods under constant energy and entrainer consumption, the best results (highest recovery of $\boldsymbol{A}$ and lowest loss of $\boldsymbol{B}$) were obtained by the mixed addition in the case studied.

Acknowledgments

This work was financially supported by the Hungarian Scientific Research Foundation ("OTKA," project No: T-034659). The authors are grateful to Professors Belkacem Benadda, Pierre Moszkowicz, and Michel Otterbein (INSA-Lyon, France) for their valuable help and support.

Notation

D = distillate molar flow rate, mol/s
F = feed flow rate of the entrainer, mol/s
f = feed plate number
h = a continuous plate number, dimensionless height
L = liquid molar flow rate, mol/s
N = number of theoretical stages
P = pressure, bar
Q = heat duty, W
R = reflux ratio
SD = amount of distillate, mol
SF = amount of feed, mol
SQ = heat, J
t = time, s
U = liquid holdup, mol
x = liquid mole fraction
y = vapor mole fraction

Greek letters

α = relative volatility
β = ratio withdrawn of the E-lean phase
Δ = difference
ϕ = molar ratio of the two liquid phases, mol/mol
η = recovery
ξ = dimensionless (warped) time

Subscripts and superscripts

A = more volatile component, low boiler
B = less volatile component, medium boiler
ch = charge
D = distillate
E = entrainer, high boiler
i = component
j = plate
R = reflux
S = still
spec = specified value
max = maximum
min = minimum
mod. = modified value
vol = volumetric
0 = overall

Literature Cited

Ahon, V. R., and J. L. de Medeiros, "Optimal Programming of Ideal and Extractive Batch Distillation: Single Vessel Operations," *Comput. Chem. Eng.*, **25**, 1115 (2001).

Bernot, C., M. Doherty, and M. F. Malone, "Patterns of Composition Change in Multicomponent Batch Distillation," *Chem. Eng. Sci.*, **45**, 1207 (1990).

Bernot, C., M. Doherty, and M. F. Malone, "Feasibility and Separation Sequencing in Multicomponent Batch Distillation," *Chem. Eng. Sci.*, **46**, 1311 (1991).

Block, U., and B. Hegner, "Development and Application of a Simulation Model for Three-Phase Distillation," *AIChE J.*, **22**, 582 (1976).

Bril, Zs. A., A. C. Mozzsuhin, F. B. Petljuk, and L. A. Serafimov, "Mathematical Modelling of the Rectification of Multicomponent Mixtures with Liquid Phase Splitting on the Plates of the Column," *Teor. Osn. Chim. Technol.*, **8**, 351 (1974).

Chemstations, "CHEMCAD User Guide," (2000).

Cheong, W. Y., and P. I. Barton, "Azeotropic Distillation in a Middle Vessel Batch Column. 1. Model Formulation and Linear Separation Boundaries," *Ind. Eng. Chem. Res.*, **38**, 1504 (1999a).

Cheong, W. Y., and P. I. Barton, "Azeotropic Distillation in a Middle Vessel Batch Column. 2. Non-Linear Separation Boundaries," *Ind. Eng. Chem. Res.*, **38**, 1531 (1999b).

Cheong, W. Y., and P. I. Barton, "Azeotropic Distillation in a Middle Vessel Batch Column. 3. Model Validation," *Ind. Eng. Chem. Res.*, **38**, 1549 (1999c).

Düssel, R., and J. Stichlmair, "Separation of Azeotropic Mixtures by Batch Distillation Using an Entrainer," *Comput. Chem. Eng.*, **19**, S113 (1995).

Düssel, R., and M. Warter, "Batch Distillation of Azeotropic Mixtures in a Regular and Inverted Batch Column," *Chem. Ing. Tech.*, **72**, 675 (2000).

Ewell, R. H., and L. M. Welch, "Rectification in Ternary Systems Containing Binary Azeotropes," *Ind. Eng. Chem.*, **37**, 1224 (1945).

Kim, K. J., and U. M. Diwekar, "New Era in Batch Distillation: Computer Aided Analysis, Optimal Design and Control," *Rev. Chem. Eng.*, **17**, 111 (2001).

Köhler, J., H. Haverkamp, and N. Schadler, "Zur Diskontinuierlichen Rektifikation Azeotroper Gemische mit Hilfsstoffeinsatz," *Chem. Ing. Tech.*, **67**, 967 (1995).

Lang, P., S. Kemeny, and J. Manczinger, "Modelling of Three Phase Distillation," Summer Meeting of Chemical Engineers and Mathematicians, Veszprem, Hungary (1985).

Lang, P., “Modeling of Countercurrent Separation Processes,” Thesis of Candidate of Science, Technical Univ. of Budapest, Dept. of Chemical Engineering, Budapest, Hungary (1991).

Lang, P., H. Yatim, P. Moszkowicz, and M. Otterbein, “Batch Extractive Distillation Under Constant Reflux Ratio,” *Comput. Chem. Eng.*, **18**, 1057 (1994).

Lang, P., G. Modla, B. Benadda, and Z. Lelkes, “Homoazeotropic Distillation of Maximum Azeotropes in a Batch Rectifier with Continuous Entrainer Feeding: I. Feasibility Studies,” *Comput. Chem. Eng.*, **24**, 1465 (2000a).

Lang P., G. Modla, B. Kotai, Z. Lelkes, and P. Moszkowicz, “Homoazeotropic Distillation of Maximum Azeotropes in a Batch Rectifier with Continuous Entrainer Feeding: II. Rigorous Simulation Results,” paper accepted for the PSE 2003, *Comput. Chem. Eng.*, **24**, 1429 (2000b).

Lang, P., G. Modla, and B. Kotai, “Batch Heteroazeotropic Rectification under Continuous Entrainer Feeding: II. Rigorous Simulation Results,” paper accepted for PSE2003 (2003).

Lelkes, Z., P. Lang, P. Moszkowicz, B. Benadda, and M. Otterbein, “Batch Extractive Distillation: The Process and the Operational Policies,” *Chem. Eng. Sci.*, **53**, 1331 (1998a).

Lelkes, Z., P. Lang, B. Benadda, and P. Moszkowicz , “Feasibility of Extractive Distillation in a Batch Rectifier,” *AIChE J.*, **44**, 810 (1998b).

Low, K. H., and E. Sorensen, “Optimal Operation of Extractive Distillation in Different Batch Configurations,” *AIChE J.*, **48**, 1034 (2002).

Milani, S. M., “Optimization of Solvent Feed Rate for Maximum Recovery of High Purity Top Product in Batch Extractive Distillation,” *Chem. Eng. Res. Des.*, **77**, 469 (1999).

Modla, G., P. Lang, B. Kotai, and K. Molnar, “Batch Heteroazeotropic Rectification under Continuous Entrainer Feeding: I. Feasibility Studies,” paper accepted for the PSE2003 (2003).

Mujtaba, I. M., “ Optimization of Batch Extractive Distillation Processes for Separating Close Boiling and Azeotropic Mixtures,” *Chem. Eng. Res. Des.*, **77**, 588 (1999).

Pham, H. N., and M. F. Doherty, “Design and Synthesis of Heterogeneous Azeotropic Distillations: II. Residue Curve Maps,” *Chem. Eng. Sci.*, **45**, 1837 (1990).

Phimister, J. R., and W. D. Seider, “Semicontinuous, Middle-Vessel, Extractive Distillation,” *Comput. Chem. Eng.*, **24**, 879 (2000).

Rodriguez-Donis, I., E. Pardillo-Fontdevilla, V. Gerbaud, and X. Joulia, “Synthesis, Experiments and Simulation of Heterogeneous Batch Distillation Processes,” *Comput. Chem. Eng.*, **25**, 799 (2001a).

Rodriguez-Donis, I., V. Gerbaud, and X. Joulia, “Entrainer Selection Rules for the Separation of Azeotropic and Close Boiling Temperature Mixtures by Heterogeneous Batch Distillation,” *Ind. Chem. Eng. Res.*, **40**, 4935 (2001b).

Rodriguez-Donis, I., V. Gerbaud, and X. Joulia, “Feasibility of Heterogeneous Batch Distillation Processes,” *AIChE J.*, **48**, 1168 (2002).

Safrit, B. T., and A. W. Westerberg, “Improved Operational Policies for Batch Extractive Distillation Columns,” *Ind. Eng. Chem. Res.*, **36**, 436 (1997).

Stichlmair, J. G., and J. R. Fair, *Distillation. Principles and Practice*, Wiley-VCH, New York (1998).

Van Dongen, D. B., and M. F. Doherty, “Design and Synthesis of Homogeneous Azeotropic Distillations. 1 Problem Formulation for a Single Distillation Column,” *Ind. Eng Chem. Res.*, **24**, 454 (1985).

Warter, M., and J. Stichlmair, “Batchwise Extractive Distillation in a Column with a Middle Vessel,” *Comput. Chem. Eng.*, **23**, S915 (1999).

Warter, J., R. Düssel, J. Stichlmair, and U. Weidlich, “Entrainerauswahl bei der kontinuierlichen und batchweisen Azeotroprektifikation,” *Chem. Ing. Tech.*, **71**, 385 (1999).

Yatim, H., P. Moszkowicz, M. Otterbein, and P. Lang, “Dynamic Simulation of a Batch Extractive Distillation Process,” *Comput. Chem. Eng.*, **17**, S57 (1993).

Manuscript received June 13, 2002, revision received Dec. 11, 2002, and final revision received Apr. 21, 2003.